The Abdus Salam International Centre for Theoretical Physics

2371-13

Advanced Workshop on Energy Transport in Low-Dimensional Systems: Achievements and Mysteries

15 - 24 October 2012

Asymmetric Heat Conduction and Negative Differential Thermal Resistance in Nonlinear Systems

Bambi HU

University of Houston, Department of Physics
Houston, TX
U.S.A.

Asymmetric Heat Conduction and Negative Differential Thermal Resistance in Nonlinear Systems

"It seems there is no problem in modern physics for which there are on record as many false starts, and as many theories which overlook some essential feature, as in the problem of the thermal conductivity of nonconducting crystals."

R.E. Peierls

Outline

I. Introduction

II. Necessary and sufficient conditions for normal and anomalous heat conduction

III. Heat conduction in the Frenkel-Kontorova model

IV. Asymmetric heat conduction

V. Negative differential thermal resistance

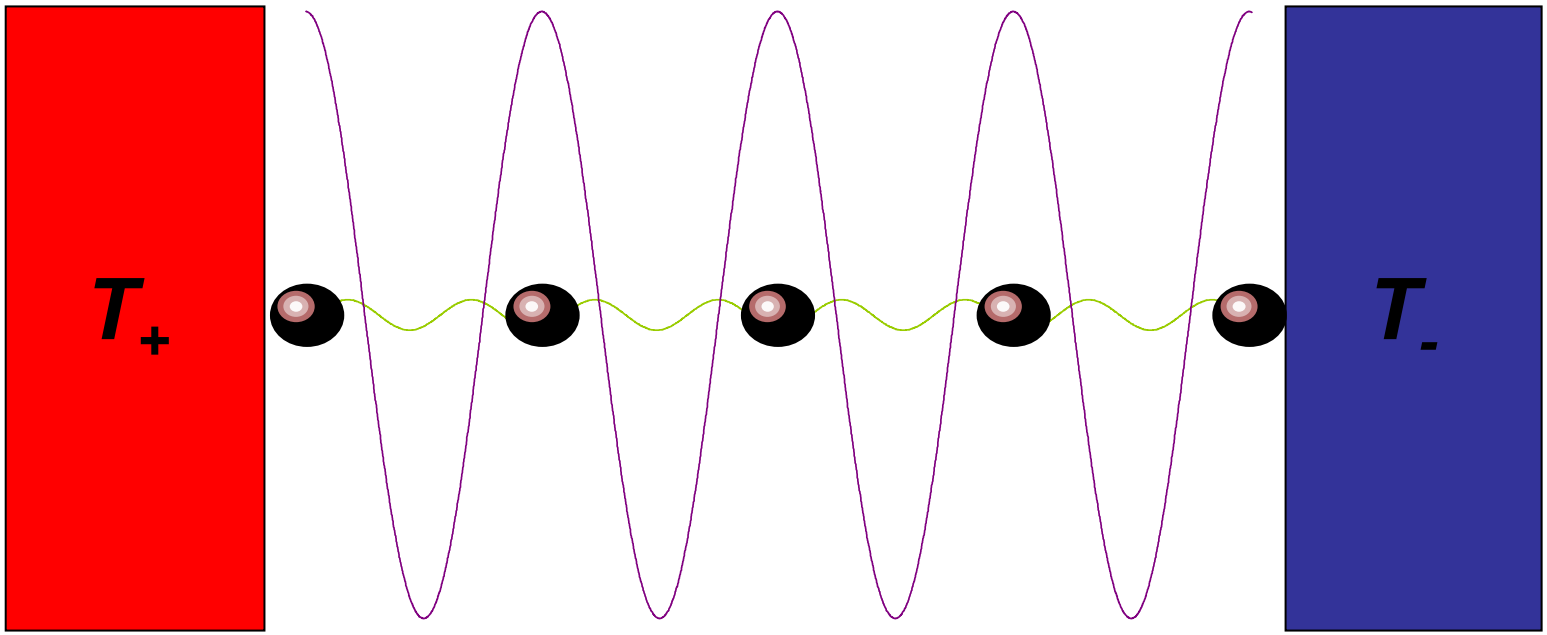
T_+
T_-

Fourier Law (1808)

$$j = -\kappa \nabla T$$

j : heat flux

∇T : temperature gradient

κ : thermal conductivity

Hamiltonian

$$H = \sum_{i=1}^{N} [\frac{p_i^2}{2m} + U(x_i) + V(x_{i+1} - x_i)]$$

$U(x_i)$: External potential

$V(x_{i+1} - x_i)$: Inter-particle potential

The crux of the heat conduction problem lies in *low dimensions*, i.e., one and two dimensions.

Green-Kubo formula

$$\kappa = \frac{1}{kT^2 d} \lim_{t\to\infty} \int_0^t d\tau \lim_{V\to\infty} \frac{1}{V} \left\langle J(\tau) \cdot J(0) \right\rangle$$

Mode coupling theory

d	$C_J(t)$	κ
1	$t^{-3/5}$	$N^{2/5}$
2	t^{-1}	$\ln N$
3	$t^{-3/2}$	finite

Some outstanding problems in heat conduction

1. First-principle derivation of the Fourier law from statistical mechanics.
2. Complete set of necessary and sufficient conditions for the validity of the Fourier law.
3. The exponent α and the problem of universality.
4. Heat conduction in two dimensions.
5. Heat conduction in three dimensions.
6. Thermal devices.
7. Quantum heat conduction.

Temperature

$$T = < \boldsymbol{u} \cdot \nabla H >$$

$$\nabla \cdot \boldsymbol{u} = 1$$

1. $\boldsymbol{u} = (0, \ldots 0, \frac{p_1}{N}, \ldots, \frac{p_N}{N})$

$$T = < \frac{\sum_{i=1}^{N} p_i^{\,2}}{Nm} >$$

2. $\boldsymbol{u} = (0, \ldots 0, p_i, 0, \ldots 0)$

$$T = < \frac{p_i^{\,2}}{m} >$$

Heat flux

$$\frac{\partial j(x,t)}{\partial x} + \frac{\partial h(x,t)}{\partial t} = 0$$

$$h(x,t) = \sum_i h_i \delta(x - x_i)$$

$$h_i = \frac{p_i^2}{2m_i} + U(x_i) + \frac{1}{2}[V(x_{i+1} - x_i) + V(x_i - x_{i-1})]$$

$$j(x,t) = \sum_i j_i \delta(x - x_i)$$

$$\frac{\partial h_i}{\partial t} = m_i \dot{x}_i \ddot{x}_i + \dot{x}_i U'(x_i) - \frac{1}{2}[(\dot{x}_{i+1} - x_i)F(x_{i+1} - x_i) + (\dot{x}_i - \dot{x}_{i-1})F(x_i - x_{i-1})]$$

$$F(x) = -V'(x) : Force$$

$$m_i \ddot{x}_i = -U'(x_i) - F(x_{i+1} - x_i) + F(x_i - x_{i-1})$$

$$\frac{\partial h_i}{\partial t} = -\frac{1}{2}[(\dot{x}_{i+1} + \dot{x}_i)F(x_{i+1} - x_i) - (\dot{x}_i + \dot{x}_{i-1})F(x_i - x_{i-1})]$$

$$j_i = \frac{1}{2} a(\dot{x}_{i+1} + \dot{x}_i)F(x_{i+1} - x_i)$$

$$\frac{j_i - j_{i-1}}{a} + \frac{\partial h_i}{\partial t} = 0$$

Density fluctuations

$$\tilde{j}(k,t) = \int dx \; j(x,t) e^{-ikx}$$

$$\tilde{h}(k,t) = \int dx \; h(x,t) e^{-ikx}$$

$$\frac{\partial \tilde{h}(k,t)}{\partial t} + ik\tilde{j}(k,t) = 0$$

$$\frac{\partial \tilde{h}}{\partial t} = \sum_i \left(\frac{\partial h_i}{\partial t} - ik\dot{x}_i h_i\right) e^{-ikx_i}$$

$$\sum_i \left(\frac{\partial h_i}{\partial t} e^{-ikx_i}\right) = \frac{1}{2}\sum_i (\phi_i - \phi_{i-1}) e^{-ikx_i} = \frac{1}{2}\sum_i \phi_i e^{-ikx_i}\left[1 - e^{-ik(x_{i+1}-x_i)}\right]$$

$$k \ll 1$$

$$\sum_i \left(\frac{\partial h_i}{\partial t} e^{-ikx_i}\right) \simeq -\frac{ik}{2}\sum_i (x_{i+1} - x_i)\phi_i e^{-ikx_i}$$

$$j_i = \frac{1}{2}(x_{i+1} - x_i)(\dot{x}_{i+1} + \dot{x}_i)F(x_{i+1} - x_i) + \dot{x}_i h_i$$

Steady state

$$\left\langle \dot{V}(q_{i+1} - q_i) \right\rangle = 0$$

$$q_i = x_i - ia$$

$$\left\langle \dot{q}_{i+1} F(q_{i+1} - q_i) \right\rangle = \left\langle \dot{q}_i F(q_{i+1} - q_i) \right\rangle$$

$$\boxed{\left\langle j_i \right\rangle = a \left\langle \dot{q}_{i+1} F(q_{i+1} - q_i) \right\rangle}$$

$$\left\langle \frac{\partial}{\partial t}(\dot{q}_i)^2 \right\rangle = 0$$

$$\left\langle \dot{q}_i F(q_{i+1} - q_i) \right\rangle = \left\langle \dot{q}_i F(q_i - q_{i-1}) \right\rangle$$

$$\left\langle j_i \right\rangle = \left\langle j_{i-1} \right\rangle = j$$

$$J = \sum_i j_i$$

Heat baths

1. Stochastic (Langevin)

$$m\ddot{q}_1 = F(q_i - q_{i-1}) - F(q_{i+1} - q_i) + (\xi_+ - \lambda_+ \dot{q}_i)\delta_{i1} + (\xi_- - \lambda_- \dot{q}_i)\delta_{iN}$$

$$\langle \xi_\pm \rangle = 0$$

$$\langle \Delta \xi_\pm^{\,2} \rangle = 2\lambda_\pm k_B T_\pm$$

$\lambda_\pm$: coupling between chain and heat bath

$$\Delta T = T_+ - T_-$$

$$\kappa = \frac{|j|L}{\Delta T}$$

2. Deterministic (Nosé-Hoover)

$$m\ddot{q}_i = F(q_i - q_{i-1}) - F(q_{i+1} - q_i) - \zeta_{\pm}\dot{q}_i$$

$$\dot{\zeta}_{\pm} = \frac{1}{\Theta_{\pm}^{\,2}}\left(\frac{1}{k_B T_{\pm} N_{\pm}} \sum_{i \in S_{\pm}} m\dot{q}_i^{\,2} - 1\right)$$

$\Theta_{\pm}$: thermostat response time

$T > T_{\pm}$, $\zeta_{\pm} > 0$;

$T < T_{\pm}$, $\zeta_{\pm} < 0$.

Necessary and sufficient conditions for normal and anomalous heat conduction

A. Integrable models

1. Linear (harmonic) models:

   Dynamics described by normal modes

2. Nonlinear but integrable models:

   Dynamics described by solitons

- Transport is ballistic rather than diffusive.
- Temperature gradient can't be established.
- κ diverges.
- Fourier's law is not obeyed.

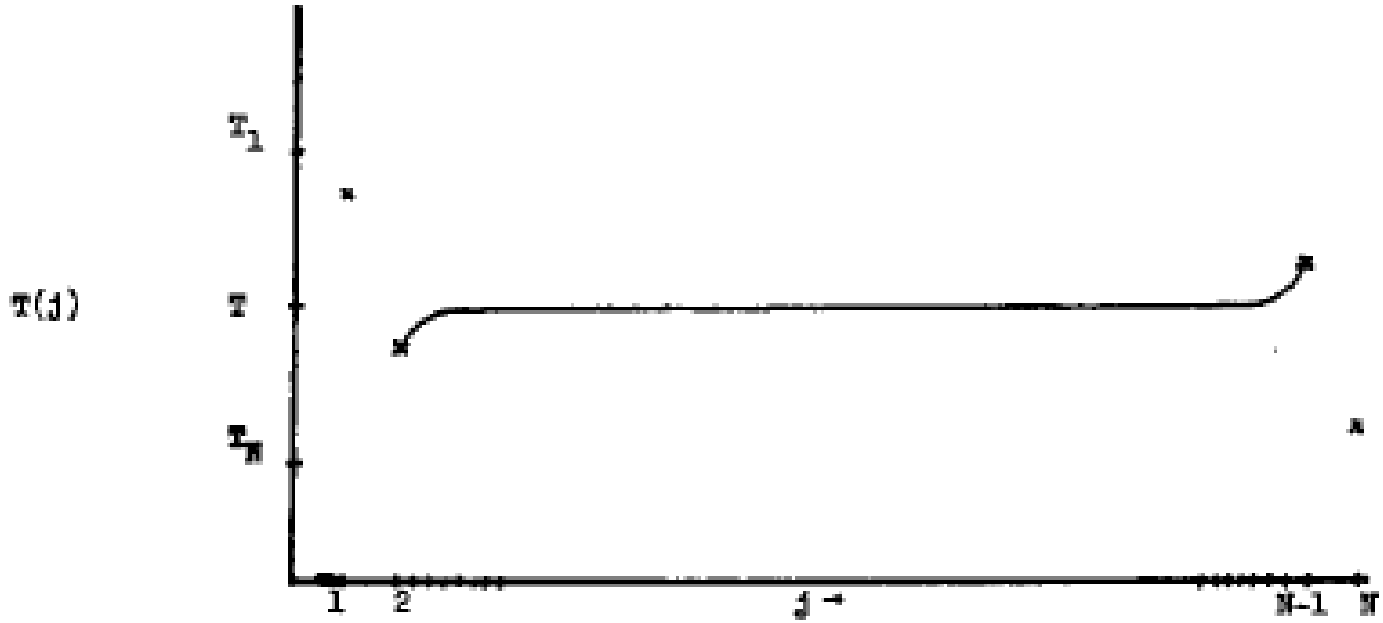

FIG. 1. Typical behavior of $T(j)$.

Z. Rieder, J. L. Lebowitz, and E. Lieb, *J. Math. Phys.* **8**, 1073 (1967).

B. Non-integrable models

1. Without an on-site potential, momentum is conserved.

Ex. Fermi-Pasta-Ulam (FPU) model

$$j \sim N^{\alpha-1}$$

$$\frac{dT}{dx} \sim N^{-1}$$

$$\kappa \sim N^{\alpha}$$

κ diverges as $N \to \infty$

Fourier' s law is not obeyed

2. With an on-site potential, momentum is not conserved.

Ex. Frenkel- Kontorova (FK) model

[B. Hu, B. Li, and H. Zhao (1998)]

$$j \sim N^{-1}$$

$$\frac{dT}{dx} \sim N^{-1}$$

$$\kappa \sim 1 \text{ (finite)}$$

Fourier's law is obeyed.

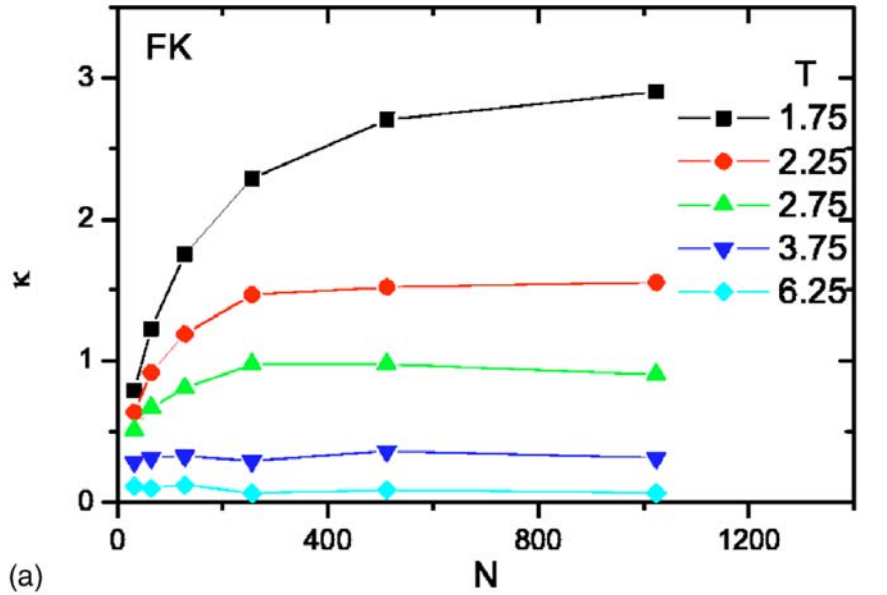

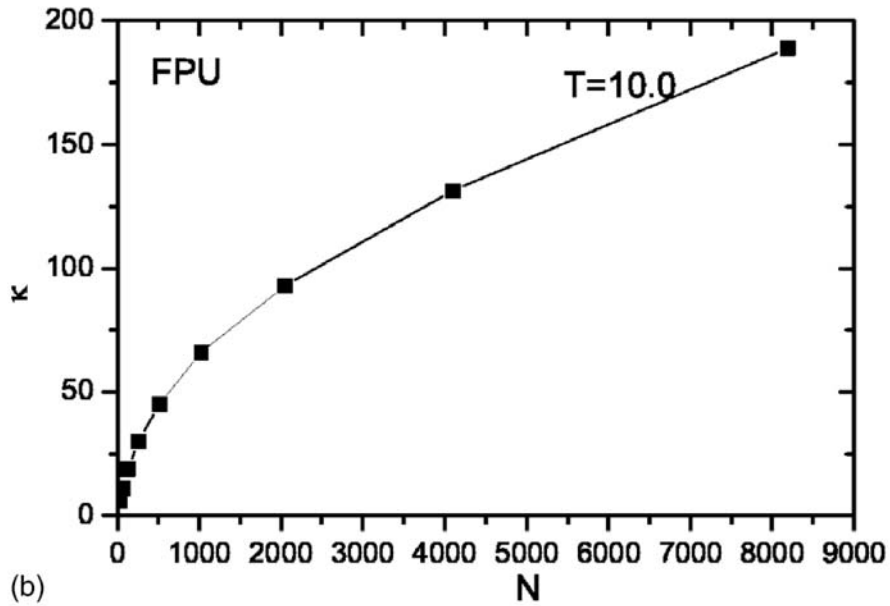

FIG. 1. Normal–normal plot of $\kappa(N)$: (a) is for the FK model, β=3.0, (b) is for the FPU model. Here, $T=(T_h+T_l)/2$.

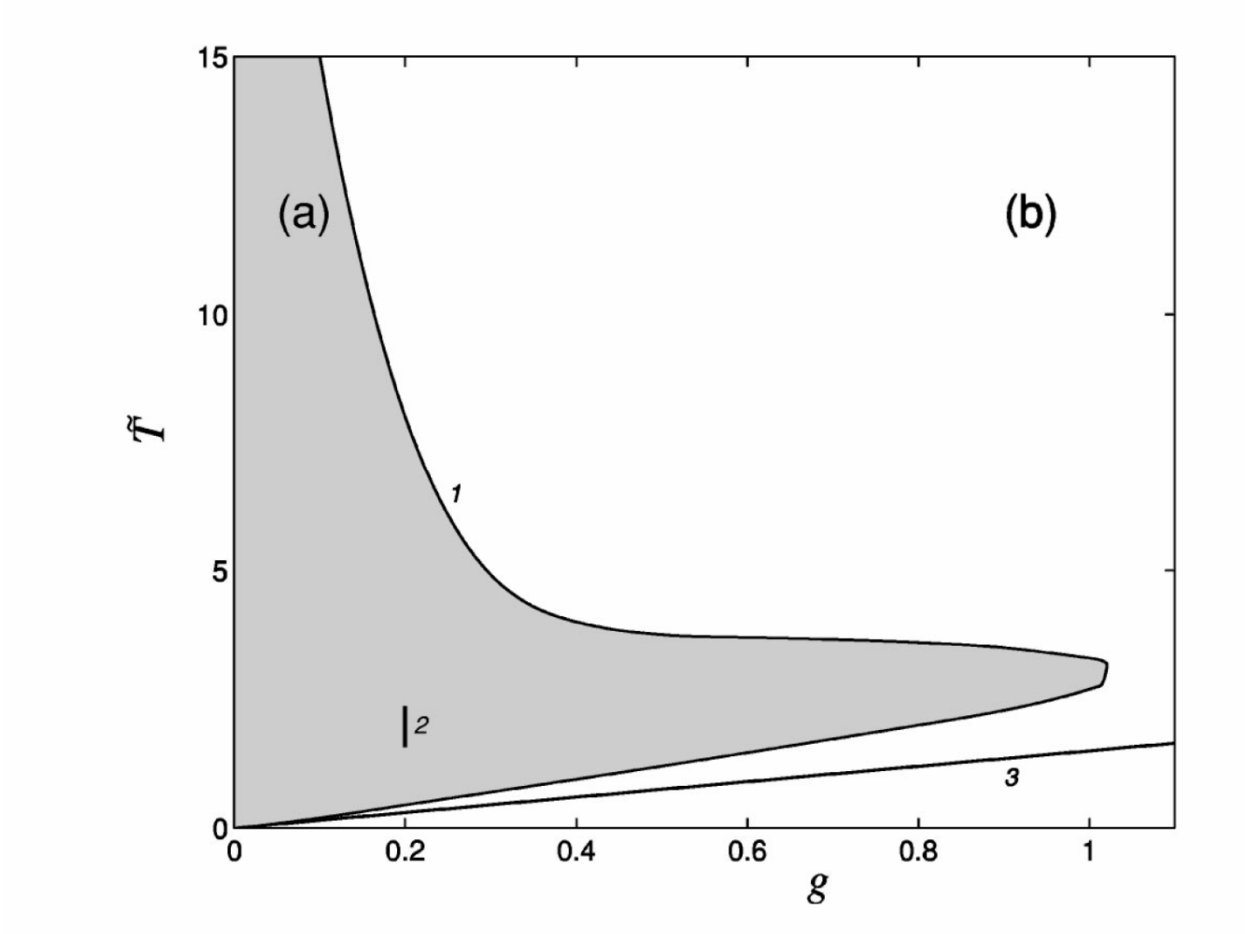

The zone in the space of parameters $(g, \tilde{T})$, where for finite chains of length $N \leq 640$ the heat conductivity converges [(a), gray zone] and diverges [(b), white zone]. Curve 1 divides these two zones. For finite chains ($N \leq 640$) finite heat conductivity is detected only above line 3.

Model		INT	DIS	CS	OP	MC	PJ	TG	HC	REM	REF
HC	Homogeneous	√				√			A		1
	Disorder	√	√			√			N	a	1,2
FPU	α			√		√			A		3
	β			√		√			A		4,5,6
Diatomic Toda				√		√		√	A	b	6,7,8
Double-well IP				√		√	√	√	A		
Disordered FPU β			√	√		√		√	N	d	9
Coupled Rotator				√		√	√	√	N		10,11
Hard point						√		√	N,A	e	12,13,14,15,16
Ding a Ling				√	√			√	N		17
Ding a Dong				√	√			√	N		18
Φ^4 model				√	√			√	N		6,19,20
FK				√	√		√	√	N	f	20,21,22
HC+SHG OP				√	√		√	√	N		22
HC+BSW OP				√	√		√	√	N		22
Billiard	Lorentz Gas			√	√			√	N		23
	Wind tree		√		√			√	N	g	24

A. Relevant factors

INT: Integrability

DIS: Disorder

CS: Chaos

OP: On-site potential

MC: Momentum conservation

PJ: Phase jump

TG: Temperature gradient

HC: Heat conduction

IP: Inter-particle potential

B. Models

HC: **Harmonic chain**

FK: $V(u) = 1 - \cos u$

SHG: **Sinh-Gordon** $V(u) = \cosh u - 1$

BSW: **Bounded single-well** $V(u) = \frac{1}{2}(1 - \operatorname{sech}^2 u)$

C. Remarks

(a) Ref. 2 claims that 2D disordered harmonic web can have a normal heat condition with sufficiently strong disorder. We have doubts.

(b) Ref. 7 claims that the diatomic Toda model can have a normal heat conduction. However, Ref. 8 gives a different conclusion.

(c) At low temperature, with the Nosé-Hoover heat bath.

(d) Ref. 13 claims that the hard-point model with alternating masses has a finite heat conduction. Ref. 14 and 15 give a different conclusion. Ref. 16 studies a modified version of the hard-point model, which can have a finite heat conduction in certain temperature regimes.

(e) Ref. 19 claims that the FK model can have normal and anomalous heat conductions in different parameters and temperature regimes.

(f) Disordered right triangle model and irrational triangle model.

D. References

1. S. Lepri, R Livi and A. Politi, Phys. Reports 377, 1 (2003).
2. L. Yang, Phys. Rev. Lett. 88, 4 (2002).
3. S. Lepri, Europhys. J. B 18, 411 (2000).
4. K. Aoki and D. Kusezov, Phys. Rev. Lett. 86, 4029 (2001).
5. S. Lepri, R Livi and A. Politi, Phys. Rev. Lett. 78, 1896 (1997).
6. B. Hu, B. W. Li, H. Zhao, Phys. Rev. E 61, 3828 (2000).
7. E. A. Jackson and A. D. Mistriotis, J. Phys.: Condens Matter 1, 1223 (1989).
8. T. Hatano, Phys. Rev. E 59, 1 (1999).
9. B. W. Li, H. Zhao, and B. Hu, Phys. Rev. Lett. 86, 63 (2001).
10. O. V. Gendelman and A. V. Savin, Phys. Rev. Lett. 84, 2381 (2000).
11. C. Giardina, R. Livi, A. Piliti and M. Vassalli, Phys. Rev. Lett. 84, 2144 (2000).
12. A. Dhar, Phys. Rev. Lett. 86, 3554 (2001).

13. P. L. Garrido, P. I. Hurtado and B. Nadrowski, Phys. Rev. Lett. 86, 5496 (2001).
14. A. Dhar, Phys. Rev. Lett. 88, 249401 (2002).
15. G. Casati and T. Prosen, Phys. Rev. E 67, 015203 (2003).
16. A. V. Savin, G. P. Tsironis and A. V. Zolotaryuk, Phys, Rev. Lett. 88, 154301 (2002).
17. G. Casati, J. Ford, F. Vivaldi and W. M. Visscher, Phys. Rev. Lett. 52, 1861 (1984).
18. T. Prosen and M. Robnik, J. Phys. A: Math Gen. 25, 3449 (1992).
19. A. V. Savin and O. V. Gendelman, Phys. Rev. E 67, 041205 (2003).
20. D. Chen, S. Aubry and G. P. Tsironis, Phys. Rev. Lett. 77, 4776 (1996).
21. B. Hu, B. W. Li, and H. Zhao, Phys. Rev. E 57, 2992 (1998).
22. G. P. Tsironis, A. R. Bishop, A. V. Savin and A. V. Zolotaryuk, Phys. Rev. E 60, 6610 (1999).
23. D. Alonso, R. Artuso, G. Casati and I. Guarneri, Phys. Rev. Lett. 82, 1859 (1999).
24. B. W. Li, L. Wang and B. Hu, Phys. Rev. Lett. 88, 223901 (2002).

A . Normal heat conduction

1. Chaos is neither a necessary nor sufficient condition
2. Necessary conditions
   (a) On-site potential or vanishing pressure
   (b) Anharmonicity
   (c) Non-integrability

B . Anomalous heat conduction

Momentum conservation is not a necessary condition but a sufficient condition provided the pressure is non-vanishing.

Exponent α

1. Renormalization group (O. Narayan and S. Ramaswamy):

$$\boxed{\alpha = \frac{1}{3}}$$

2. Mode coupling (S. Lepri, R. Livi, and A. Politi):

$$\boxed{\alpha = \frac{2}{5}}$$

Table 1
The estimated exponent α of divergence of the conductivity with size N, as obtained from both non-equilibrium molecular dynamics (NEMD) simulations and through Green–Kubo (GK) equilibrium studies. Only the significative digits are reported as given in the quoted references

Model	Reference	α (NEMD)	α (GK)
FPU-β	[84,72]	0.37	0.37
FPU-α	[63]	$\lesssim 0.44$	—
Diatomic FPU $r = 2$	[86]	0.43	Compatible
Diatomic Toda $r = 2$	[85]	0.35–0.37	0.35
	[86]	0.39	Compatible
Diatomic Toda $r = 8$	[86]	0.44	Compatible
Diatomic hard points	[85]	0.35	—

Heat conduction in the Frenkel-Kontorova model

Frenkel-Kontorova (FK) model

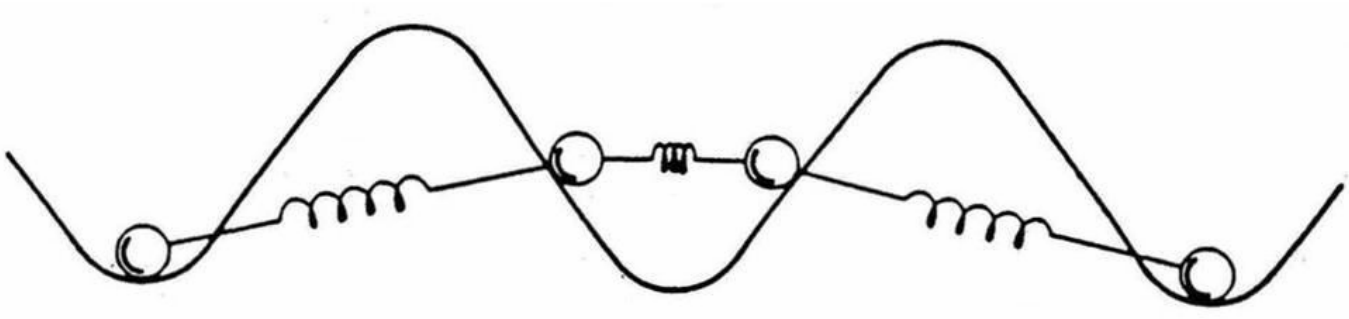

$$H = \sum_n [V(u_n) + W(u_n - u_{n-1})]$$

$V(u_n)$: external potential

$W(u_n - u_{n-1})$: spring potential

Standard FK (1938)

$$\begin{cases} W(u_n - u_{n-1}) = \dfrac{1}{2}(u_n - u_{n-1} - a)^2 \\ V(u_n) = \dfrac{k}{(2\pi)^2}(1 - \cos 2\pi u_n) \end{cases}$$

a: natural length of spring

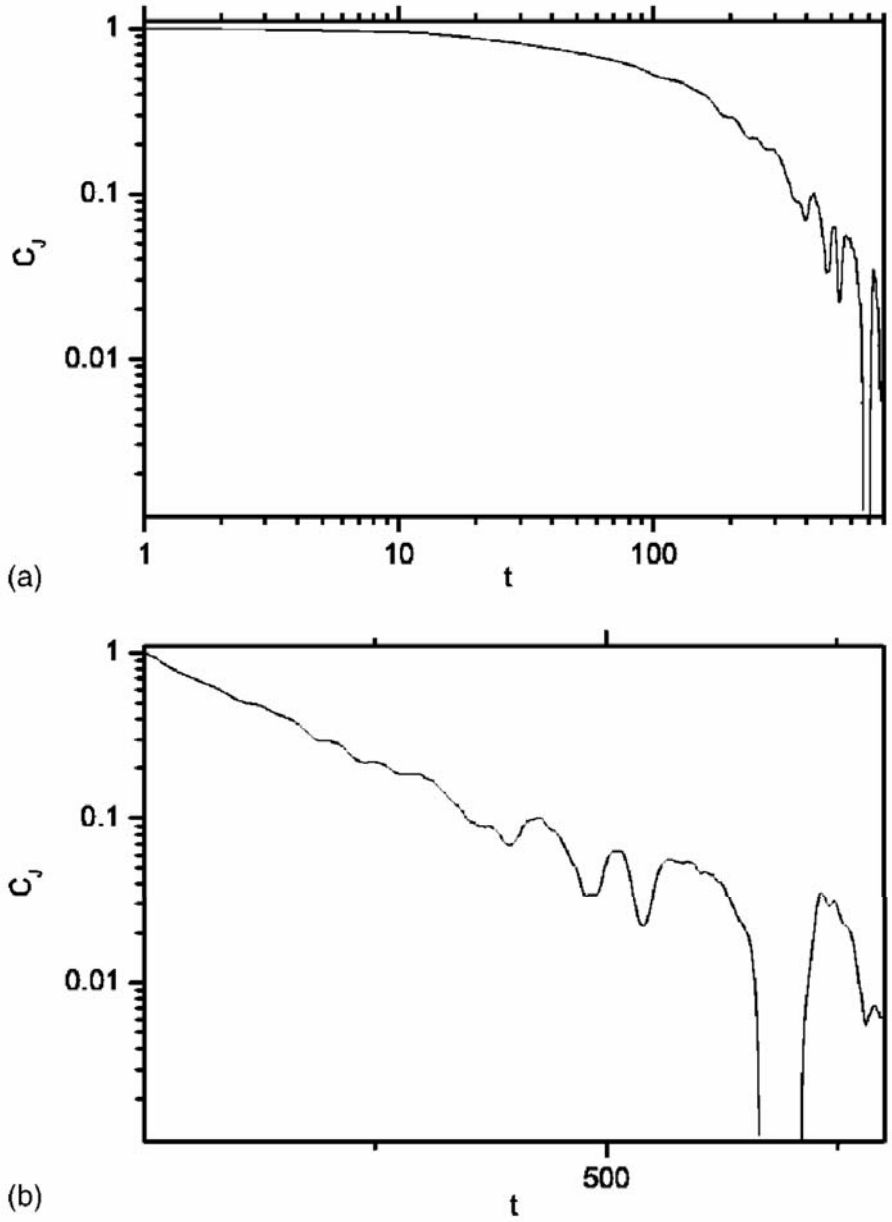

FIG. 2. (a) Log–log plot of the heat flux correlation function $C_J(t) = \langle J(t)J(0)\rangle$; (b) plot of $C_J(t)$. $N=4096$, $T=0.5$.

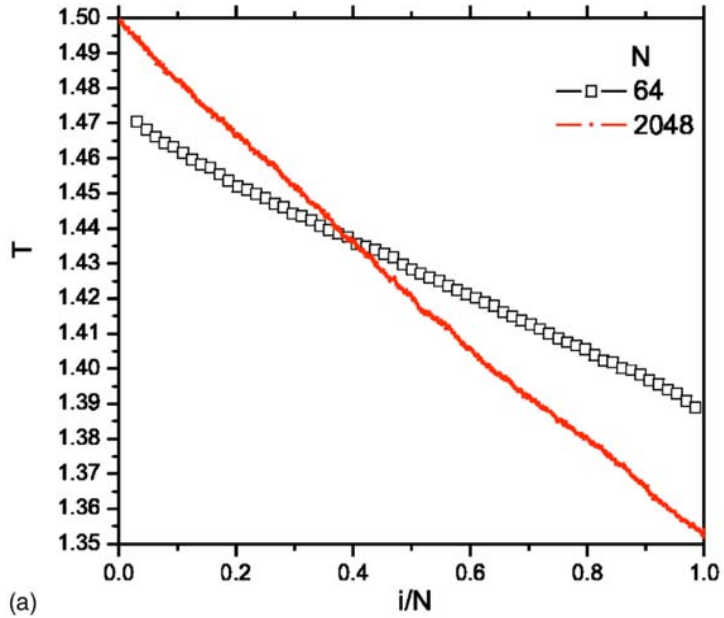

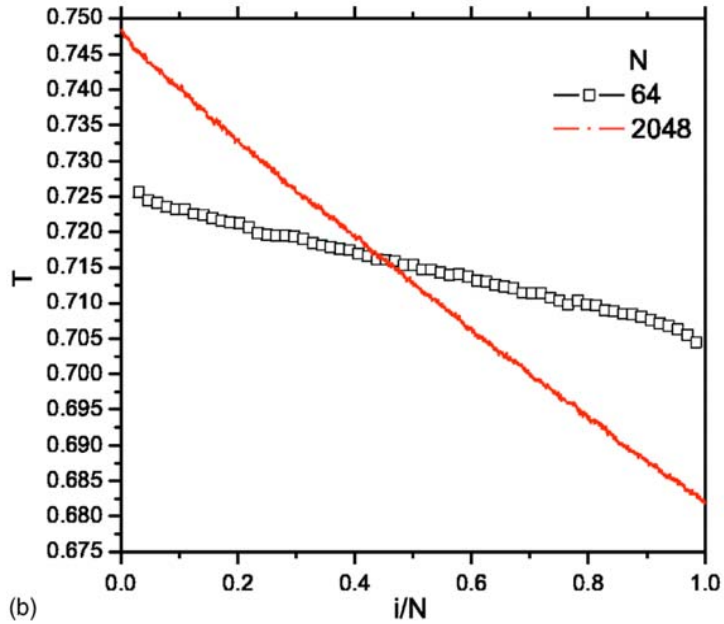

FIG. 3. Two temperature profiles.

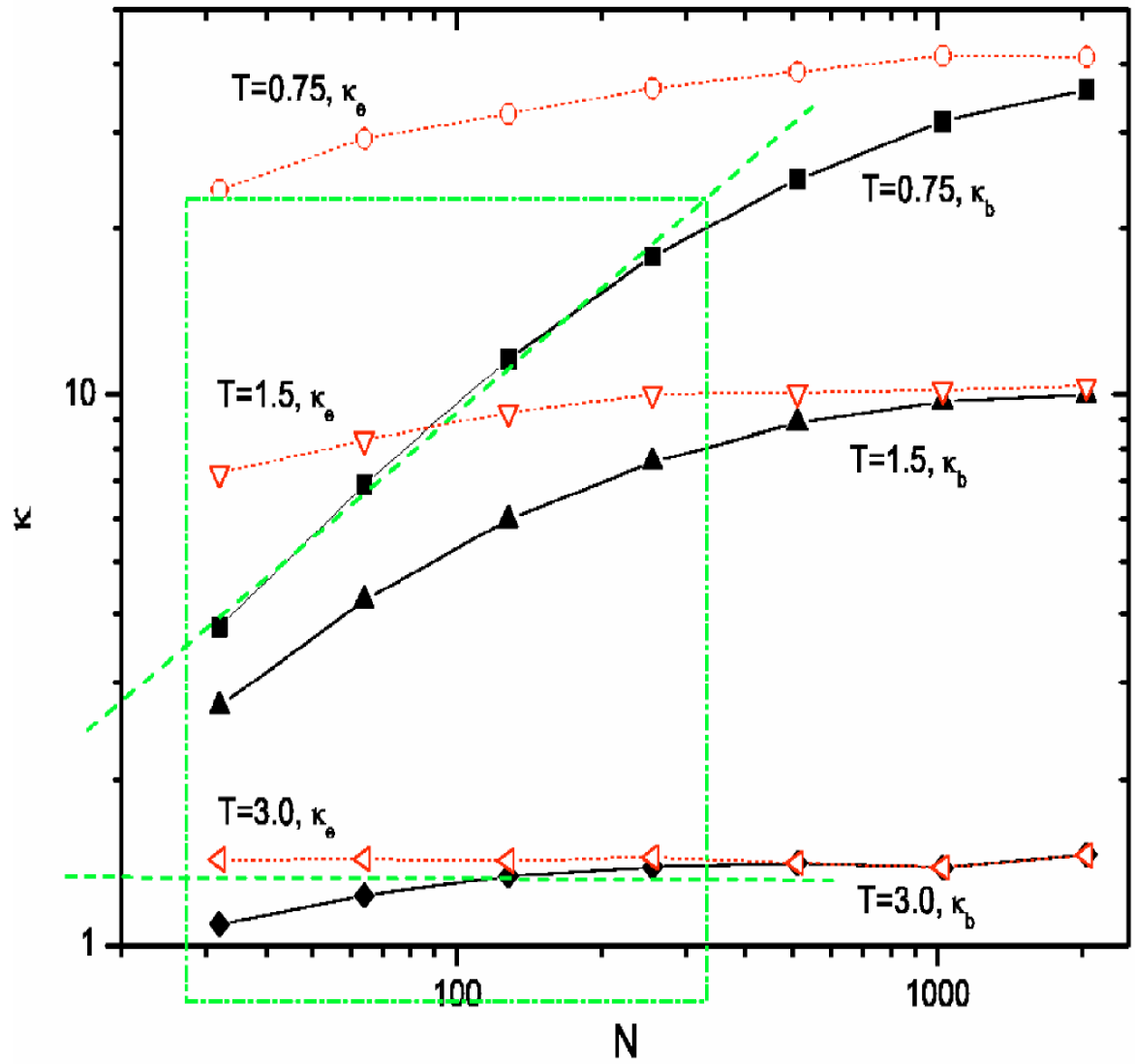

FIG. 4. Log–log plot of $\kappa(N)$.

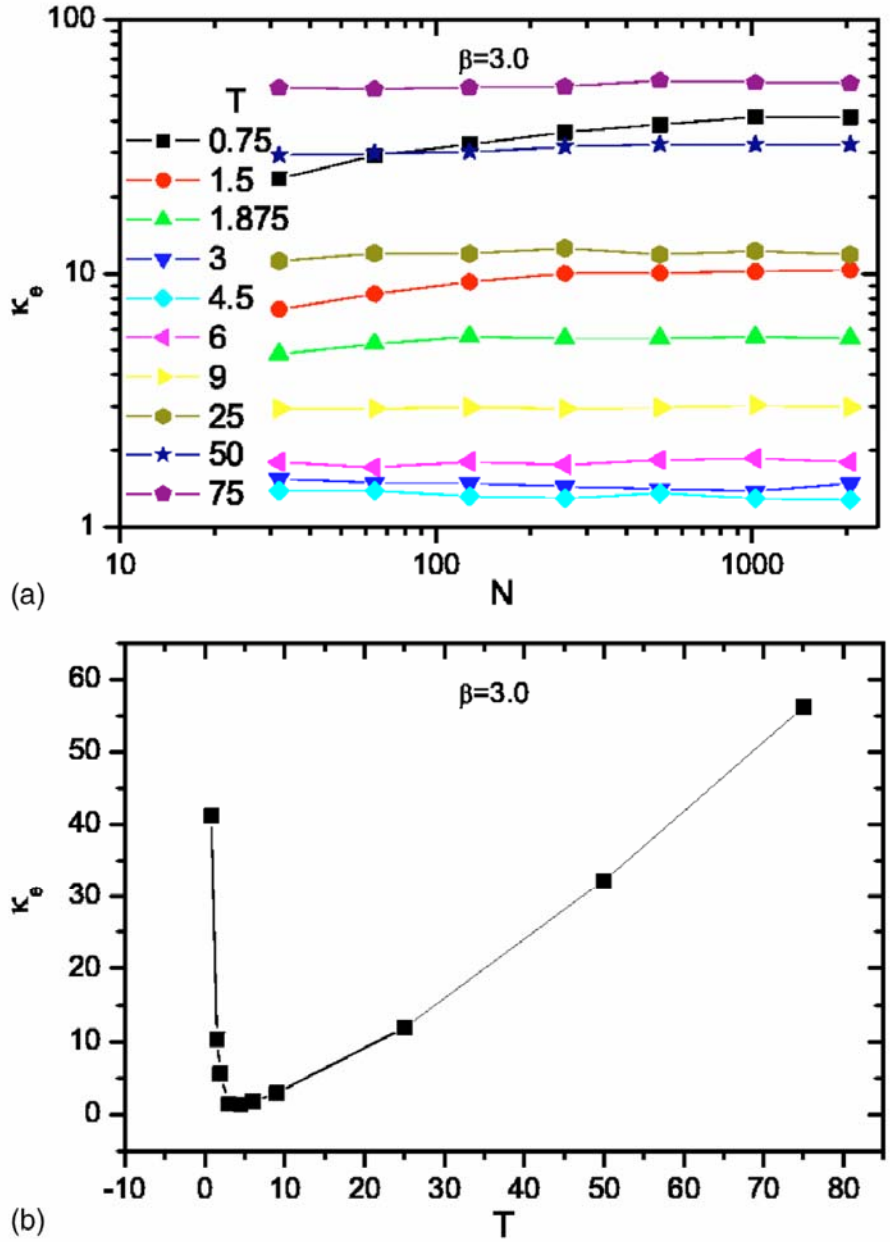

FIG. 5. (a) Log–log plot of $\kappa_e(N)$. (b) Plot of $\kappa_e(T)$.

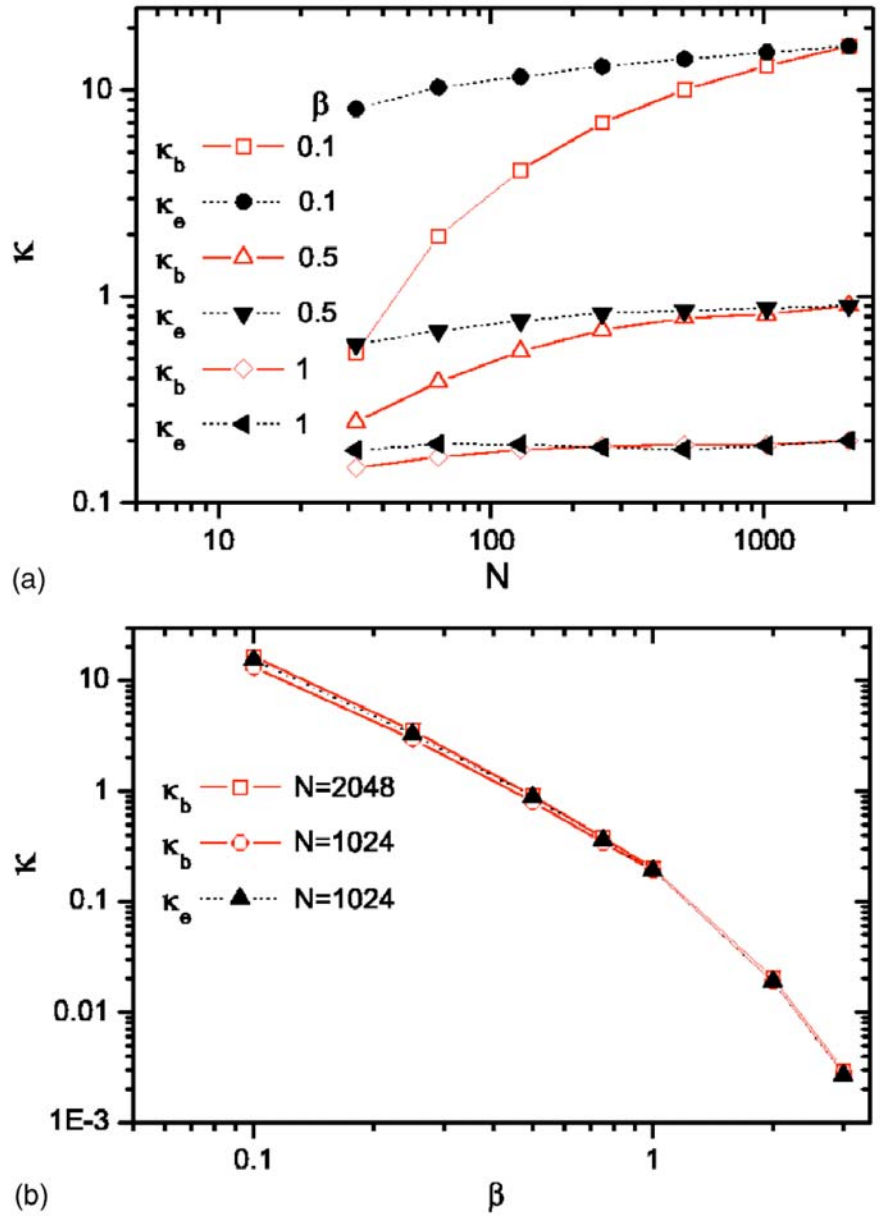

FIG. 6. (a) Log–log plot of $\kappa_e(N)$ and $\kappa_b(N)$. (b) Log–log plot of $\kappa_e(\beta)$ and $\kappa_b(\beta)$. β varies from 0.1 to 3.0. T_h=1.0, T_l=0.9.

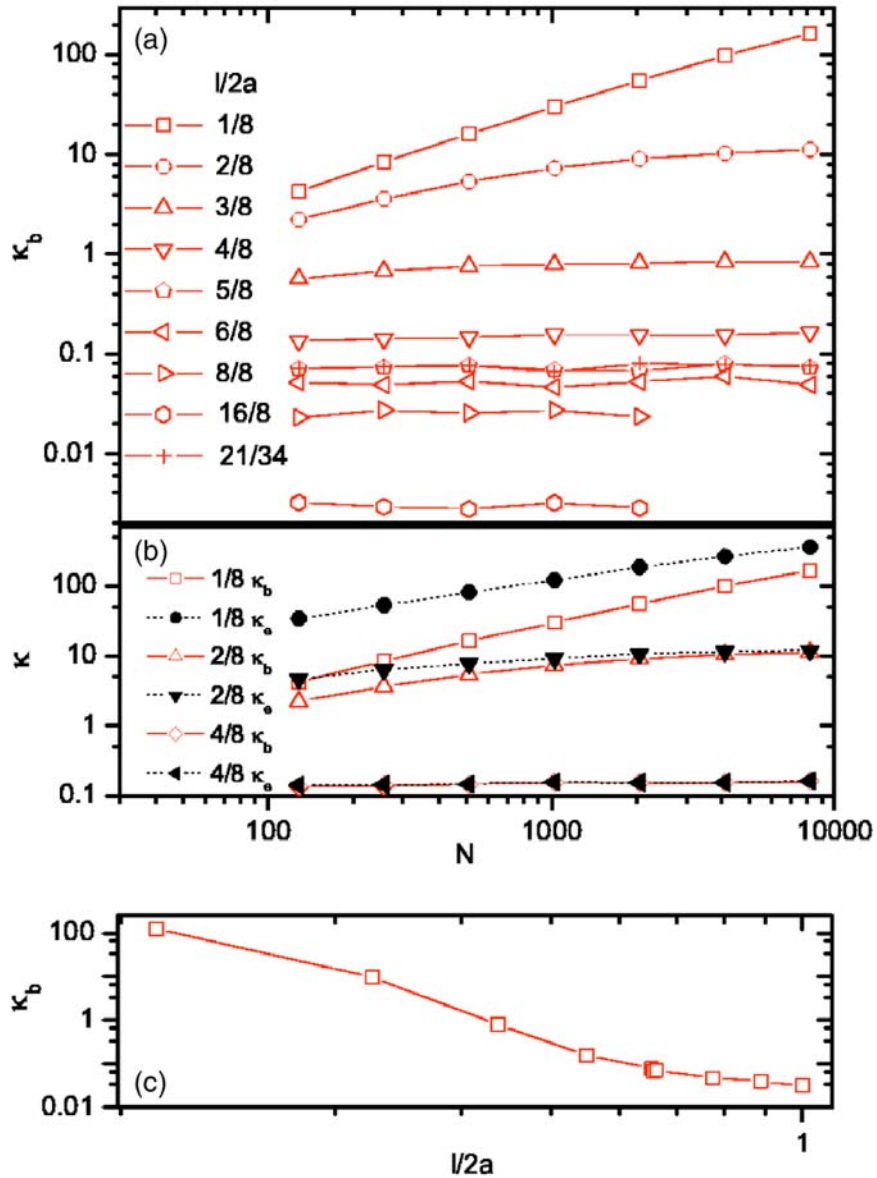

FIG. 7. Log–log plot of $\kappa(N)$ and $\kappa(\beta)$. T_h=1.0, T_l=0.9, β=2.0, and N varies from 128 to 8192. (a), (b) $\kappa_b(N)$ and $\kappa_e(N)$ for different $l/2a$; (c) $\kappa_b(l/2a)$ for N=2048.

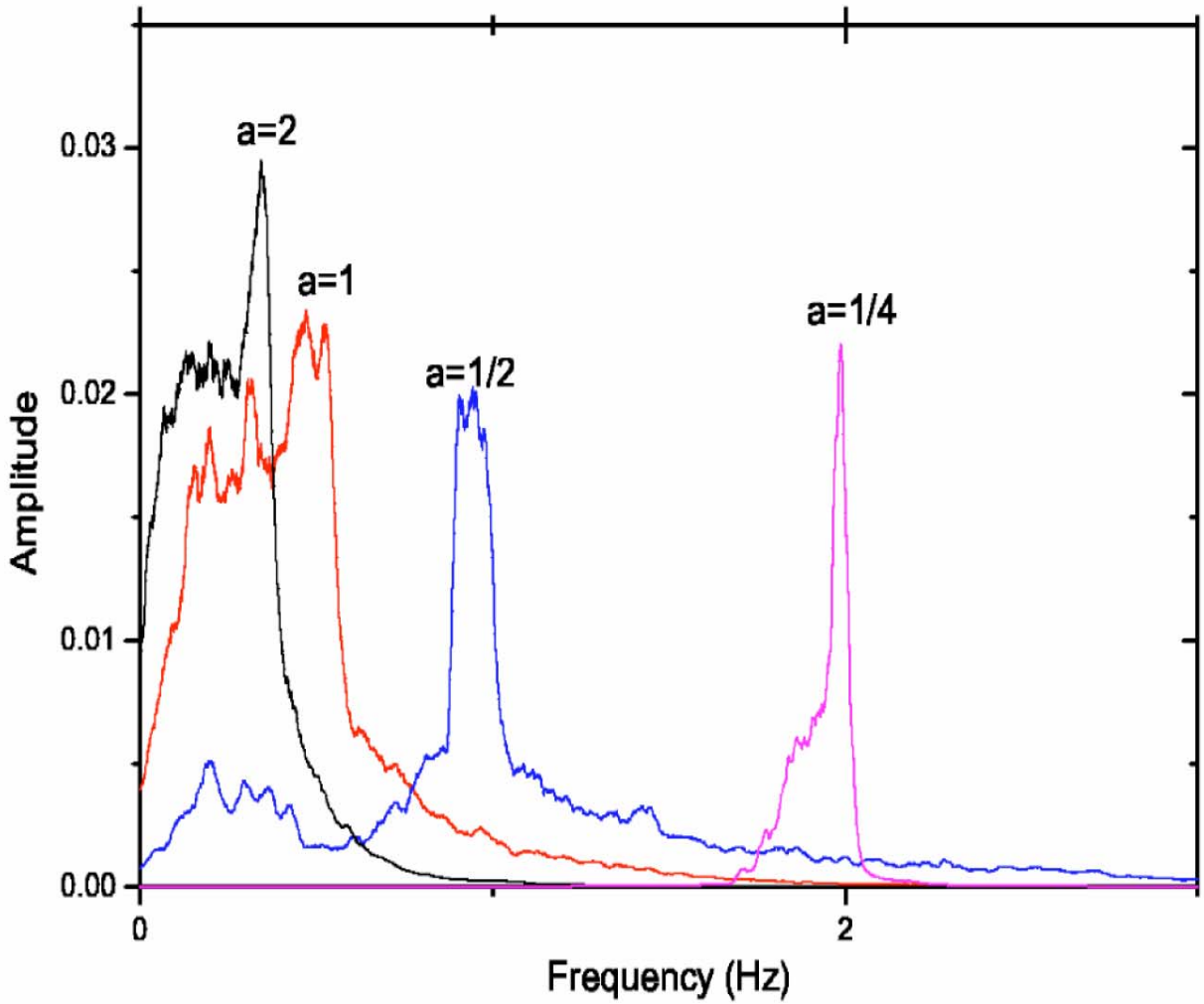

FIG. 8. Frequency spectra of particle vibrations for different a.

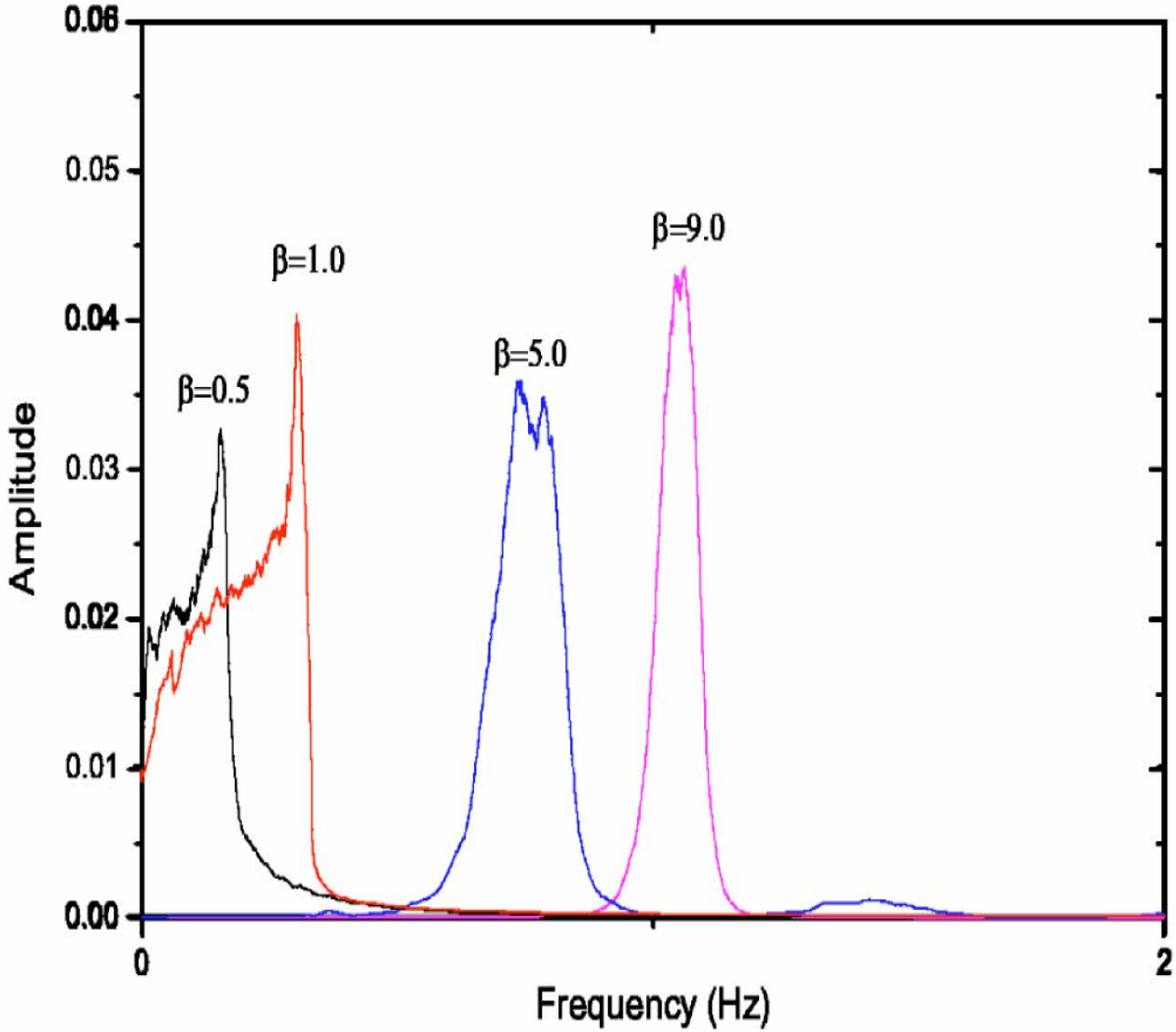

FIG. 9. Frequency spectra of particle vibrations for different β. N=256.

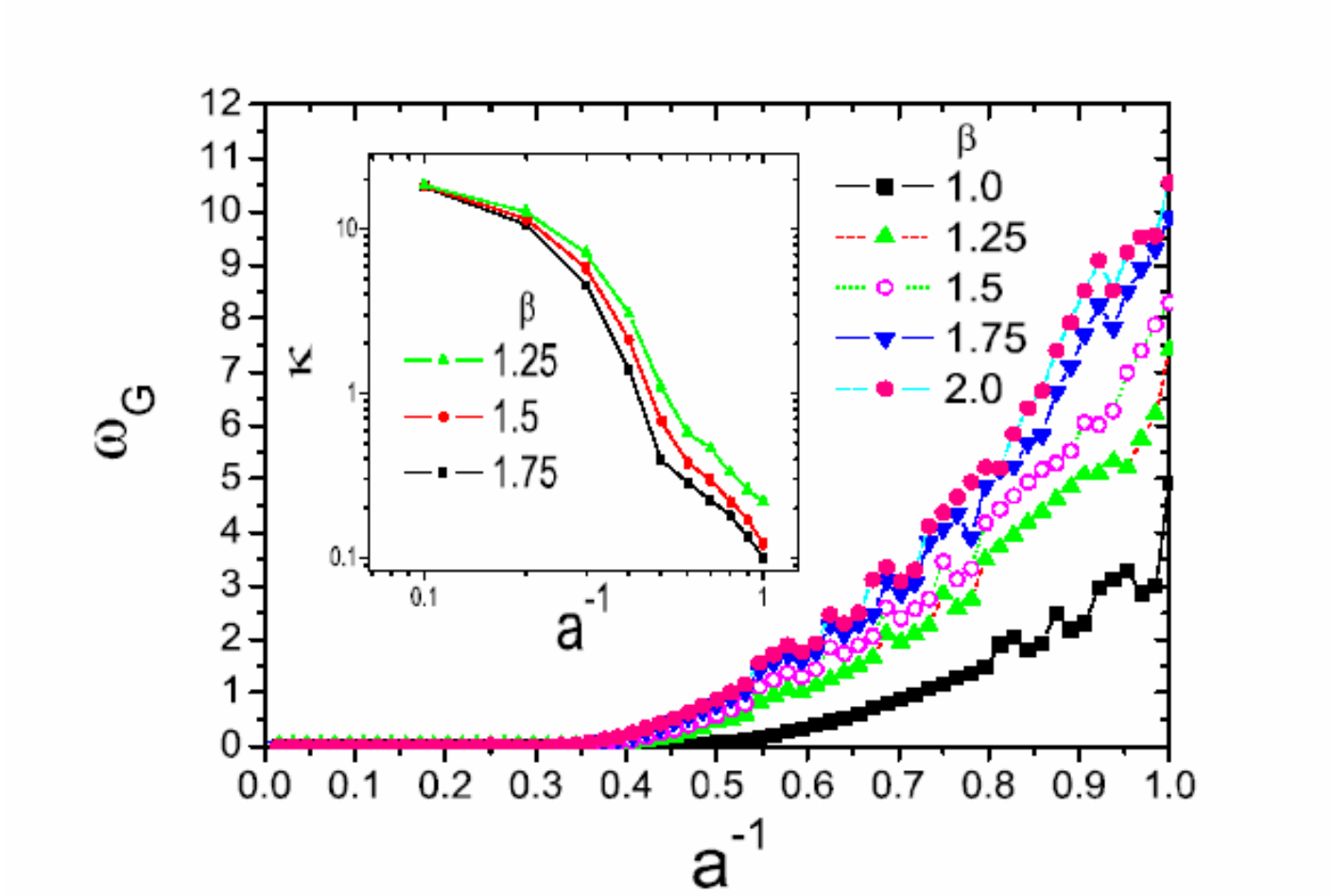

Fig. 10. Log-log of the phonon gap $\omega_{\mathrm{G}}(a,\beta)$. The inset shows the log-log plot of the thermal conductivity $\kappa(a,\beta)$. $\omega_{\mathrm{G}}(a,\beta)$ is a decreasing function of a and an increasing function of β. $\kappa(a,\beta)$ is an increasing function of a and a decreasing function of β.

Asymmetric Heat Conduction

Two-segment FK model

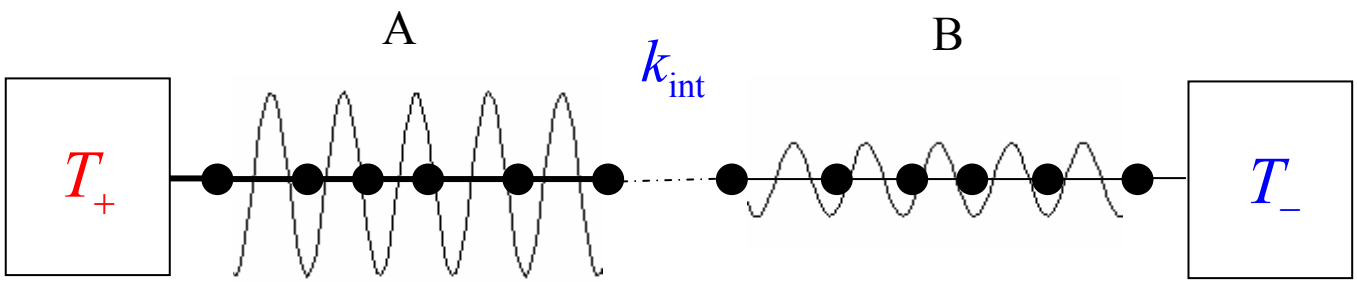

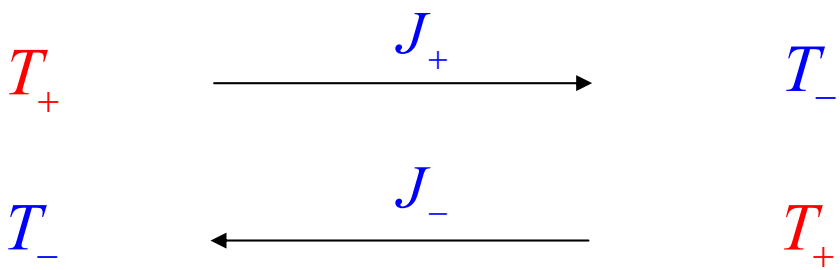

Asymmetric heat conduction: $J_+ \neq J_-$

Hamiltonian

$$H = H_A + H_B + \frac{1}{2} k_{\text{int}} (x_{N/2+1} - x_{N/2} - a)^2,$$

$$H_{A,B} = \sum_i \frac{p_i^2}{2m} + \frac{1}{2} k_{A,B} (x_{i+1} - x_i - a)^2 - \frac{V_{A,B}}{(2\pi)^2} \cos 2\pi x_i.$$

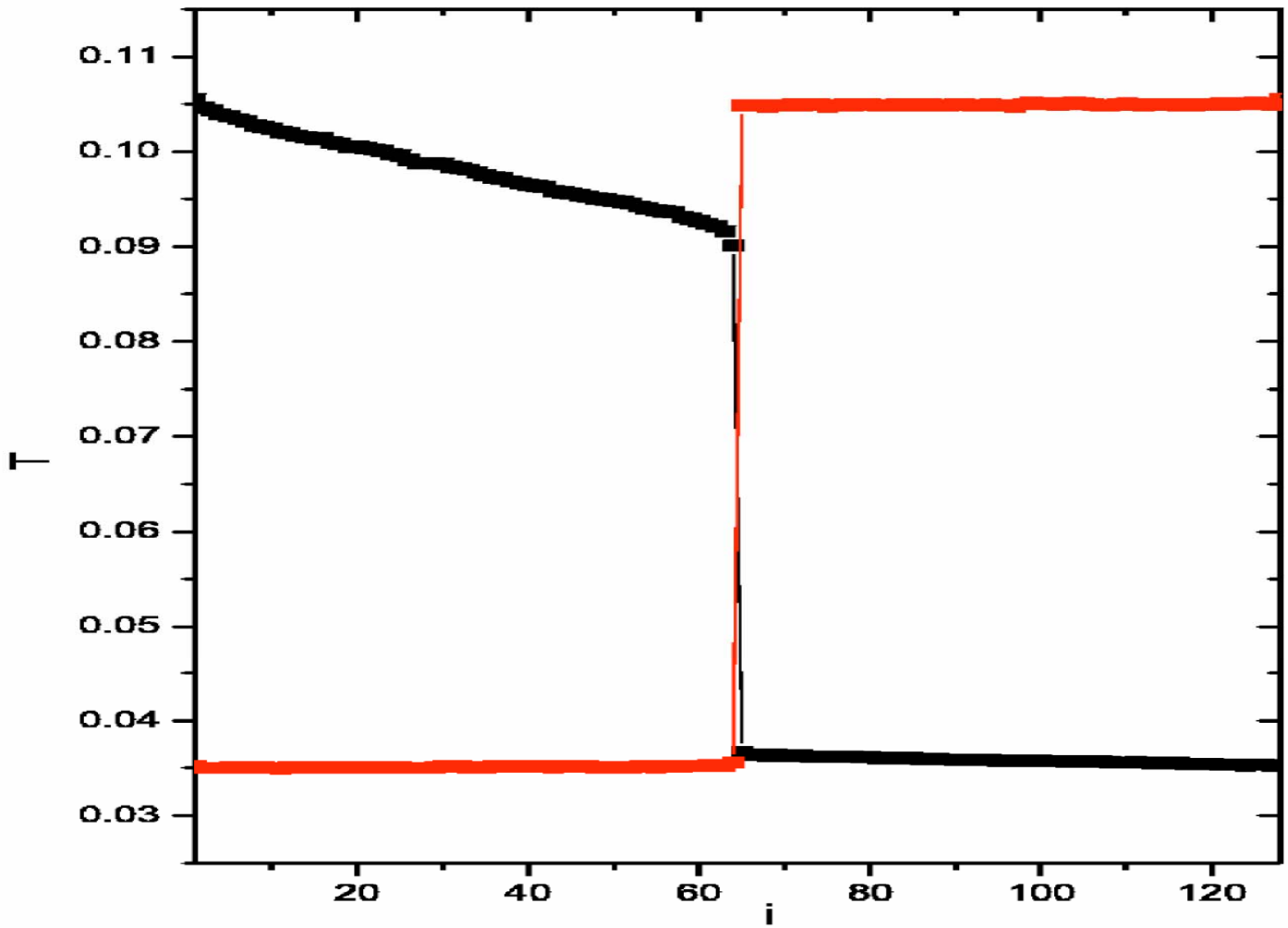

FIG. 11. Temperature profiles of the diode model.

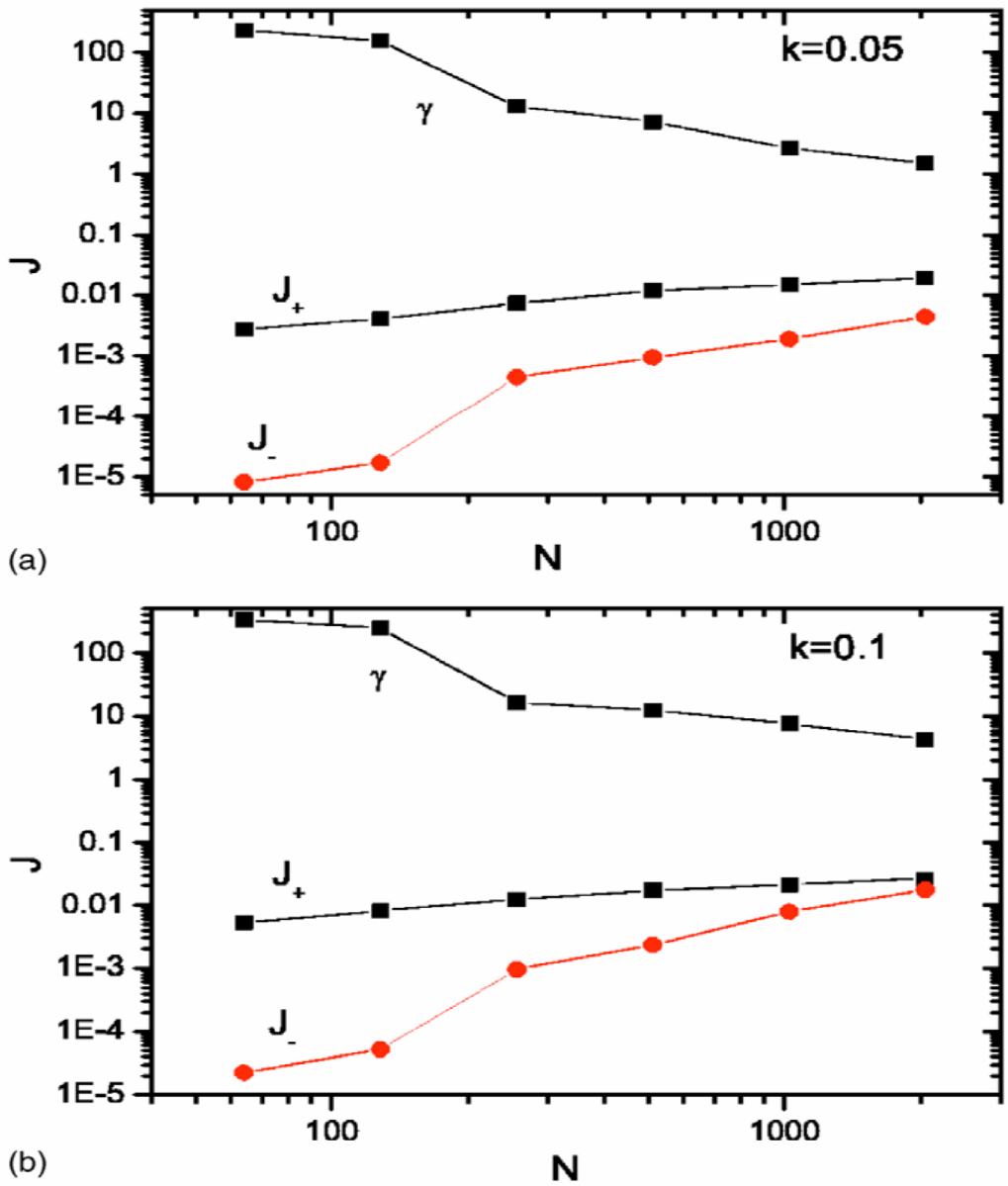

FIG. 12. Log–log plot of the total positive heat flux $J_+(N)$, the total negative heat flux $J_-(N)$, and their ratio $\gamma=|J_+(N)/J_-(N)|$ on the diode model.

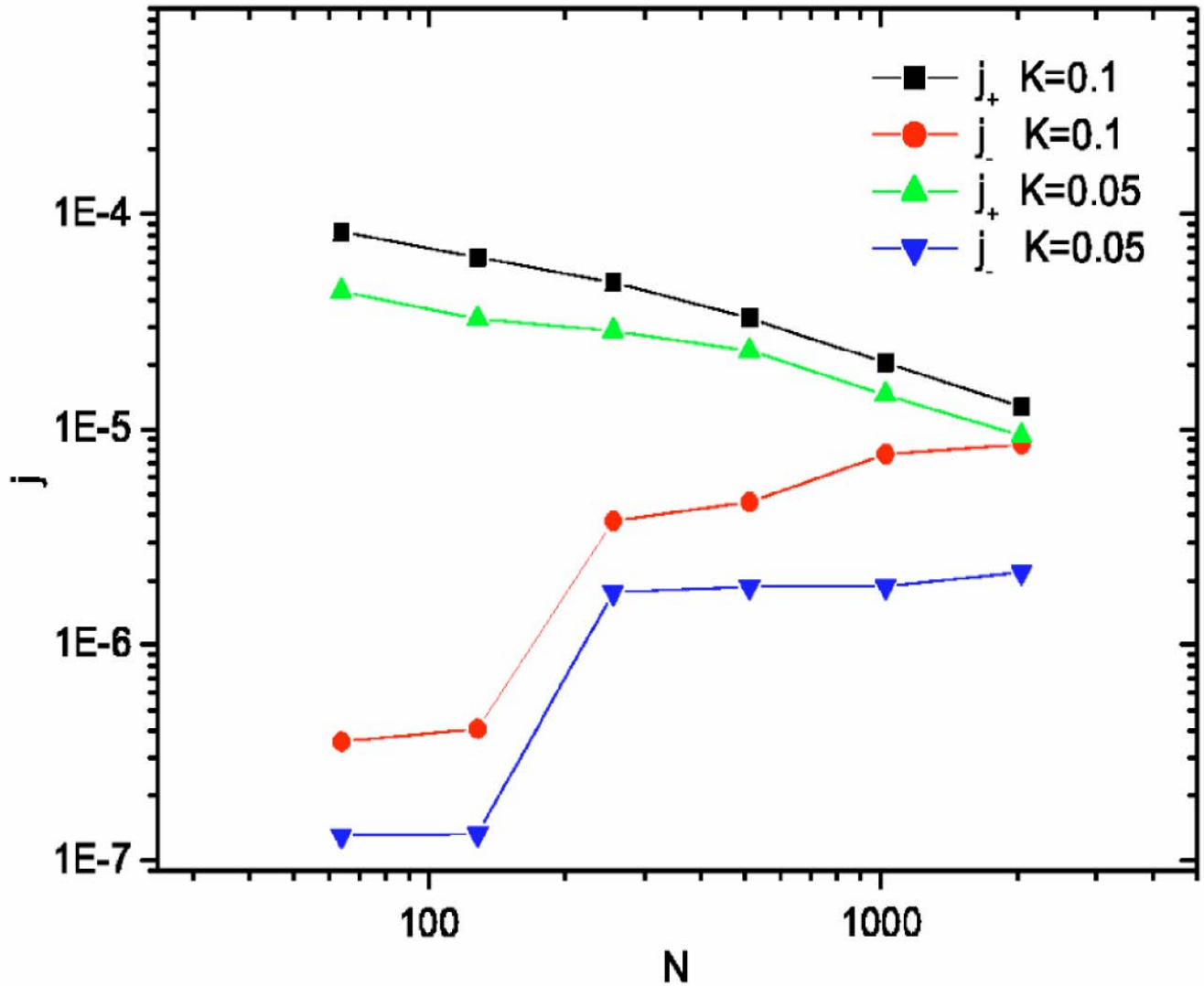

FIG. 13. Log–log plot of the positive heat flux $j_+(N)$, the negative heat flux $j_-(N)$.

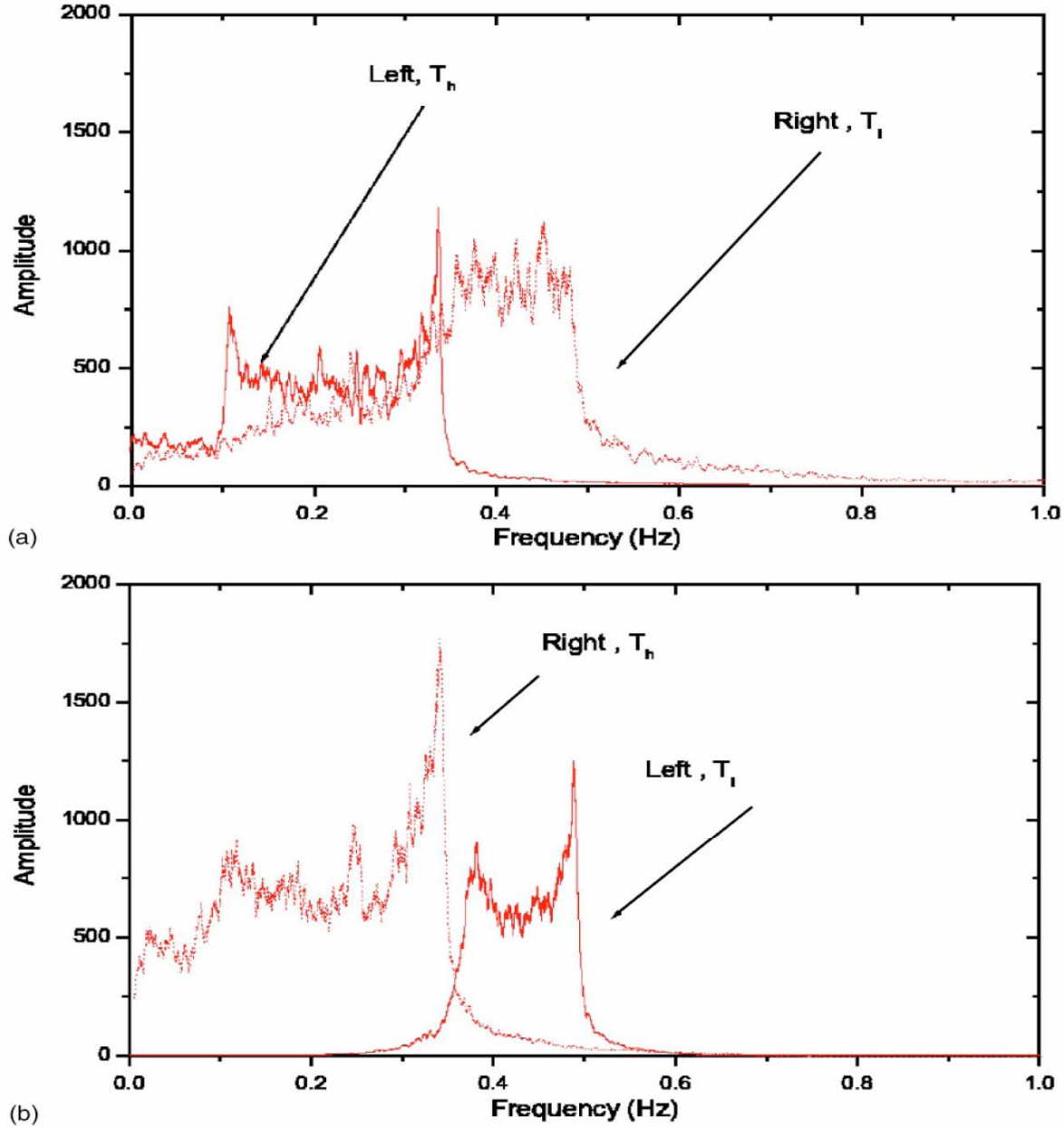

FIG. 14. Frequency spectra of particle vibrations in the diode model. $N = 256$.

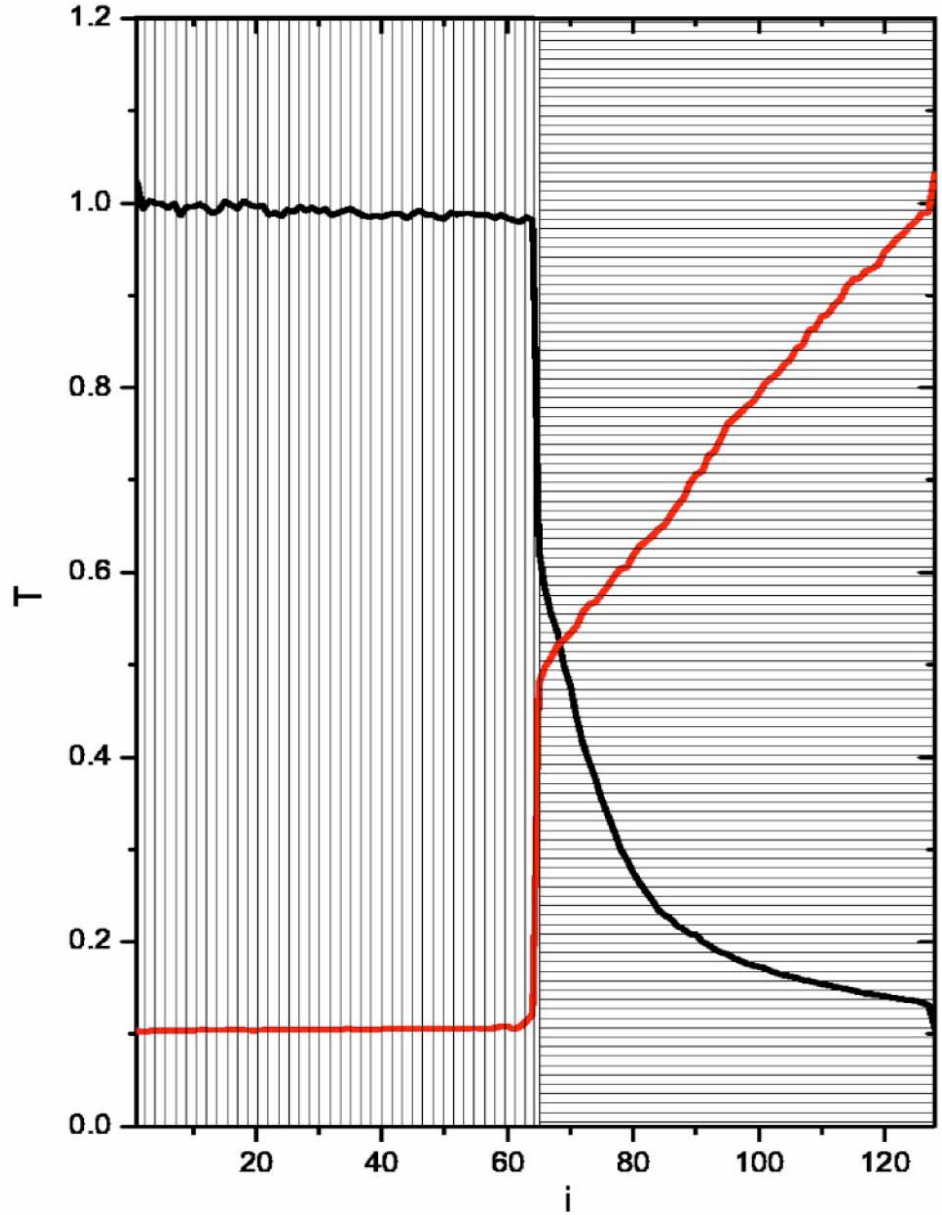

FIG. 15. Temperature profiles of the rectifier model (6). $N=128$.

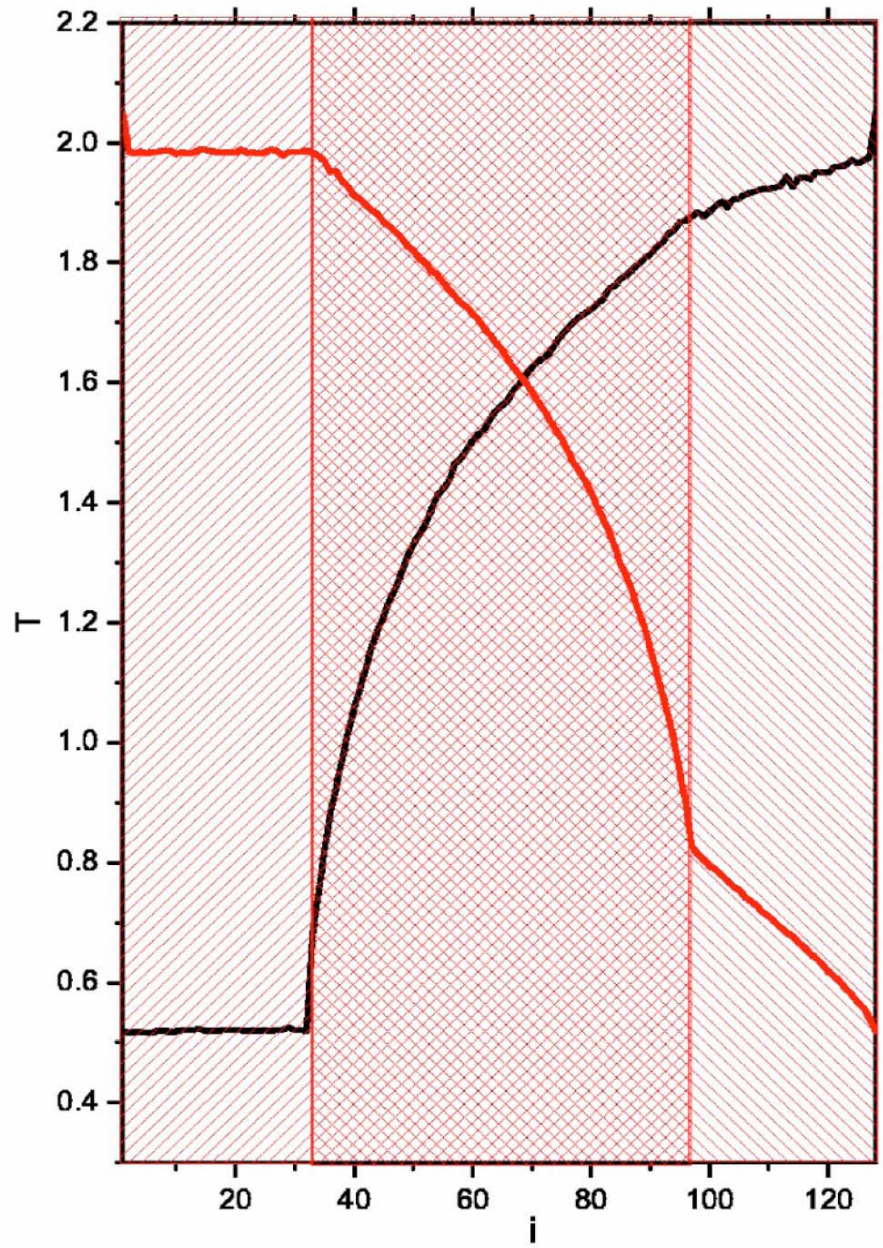

FIG. 16. Temperature profiles of the rectifier model (7). $N=128$.

- Numerical results

$$J_+ > J_- \quad \text{and} \quad J_+ / J_- \approx 100$$

- Theoretical analysis

1. Temperature-dependent phonon spectra

Low temperature limit: $\sqrt{V} < \omega < \sqrt{V + 4k}$

High temperature limit: $0 < \omega < 2\sqrt{k}$

2. Overlap/separation of phonon bands

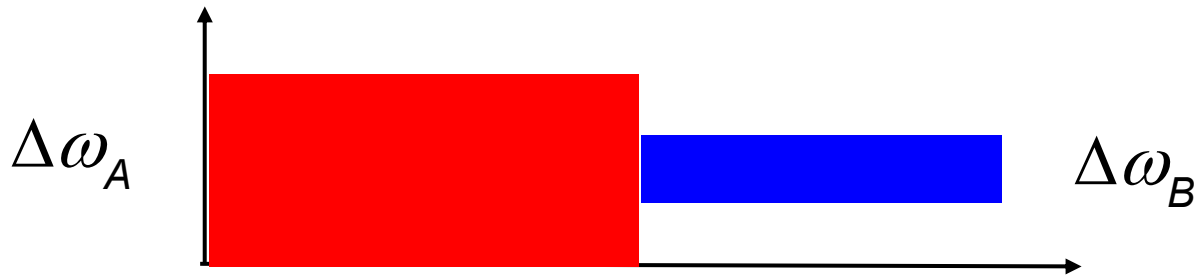
$\Delta\omega_A$
$\Delta\omega_B$

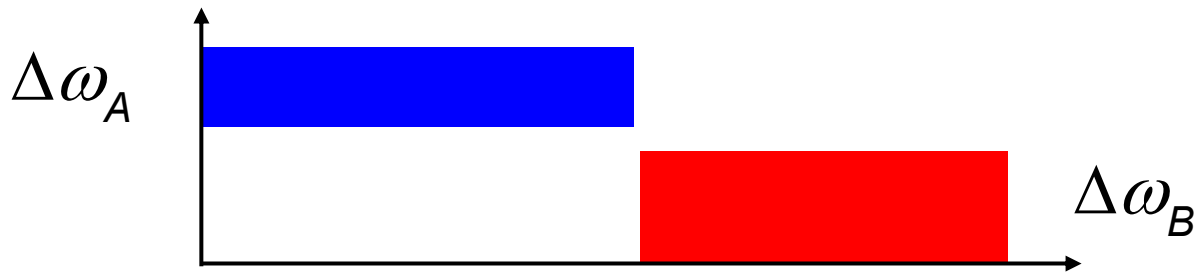
$\Delta\omega_A$
$\Delta\omega_B$

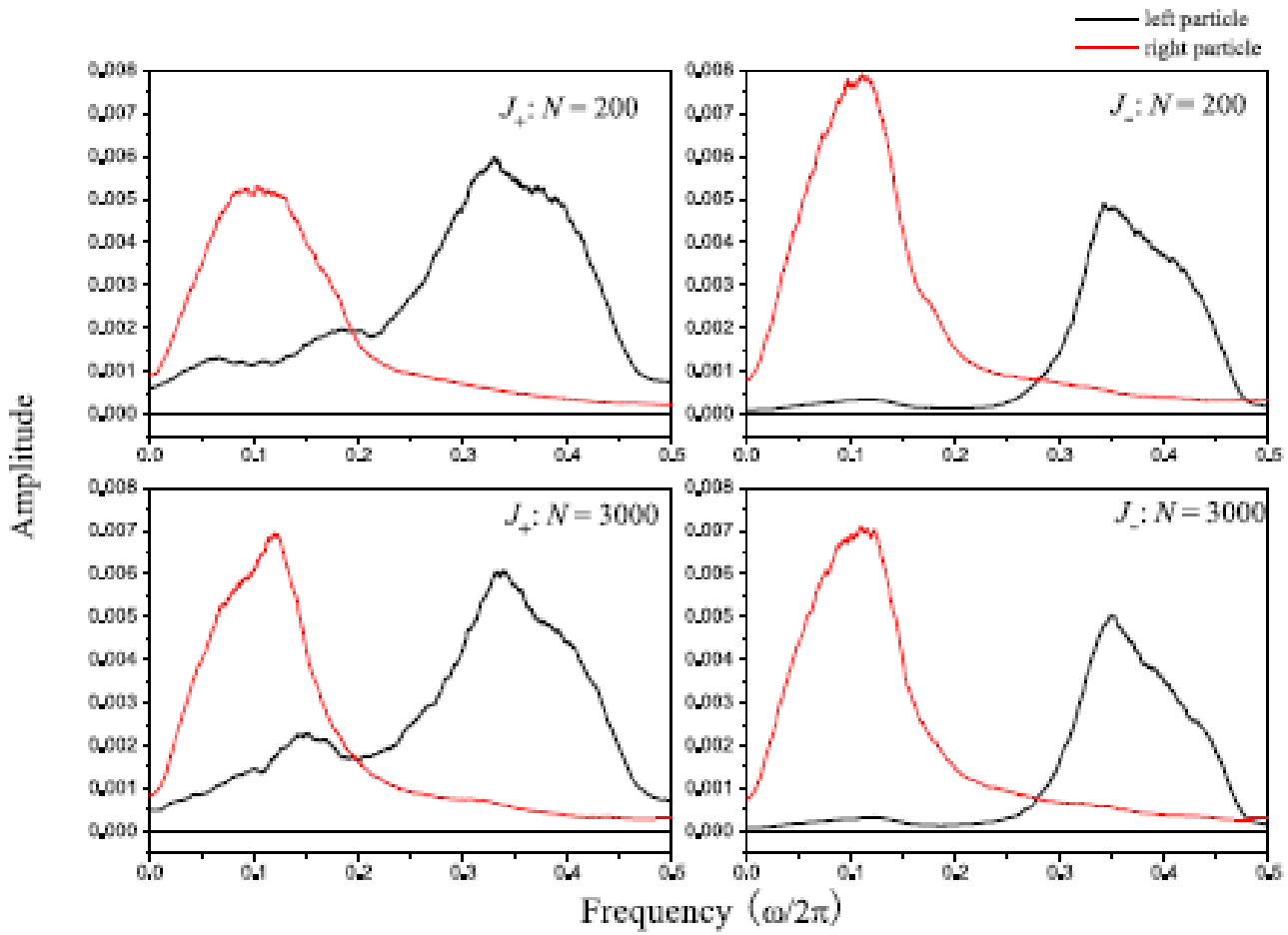

FIG. 1 (color online). Single-particle frequency spectrum of the two coupled particles ($k_{\text{int}} = 0.2$) on the left (solid line) and the right (dotted line) of the interface for $N = 200$ and $N = 3000$.

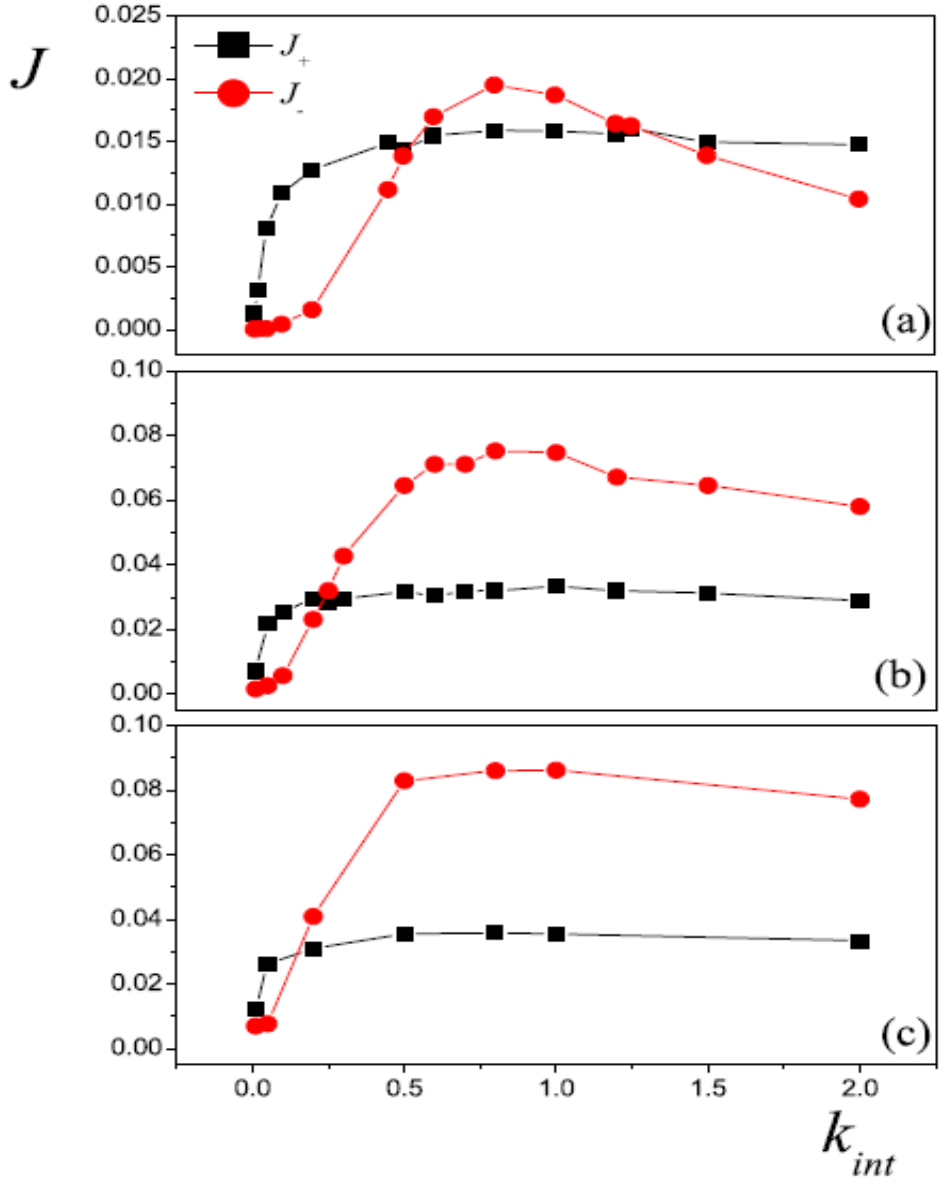

FIG. 2 (color online). Dependence of the total heat flux $J_{\pm}$ on the interfacial harmonic coupling strength k_{int} for (a) $N = 100$, (b) $N = 1000$, and (c) $N = 2000$.

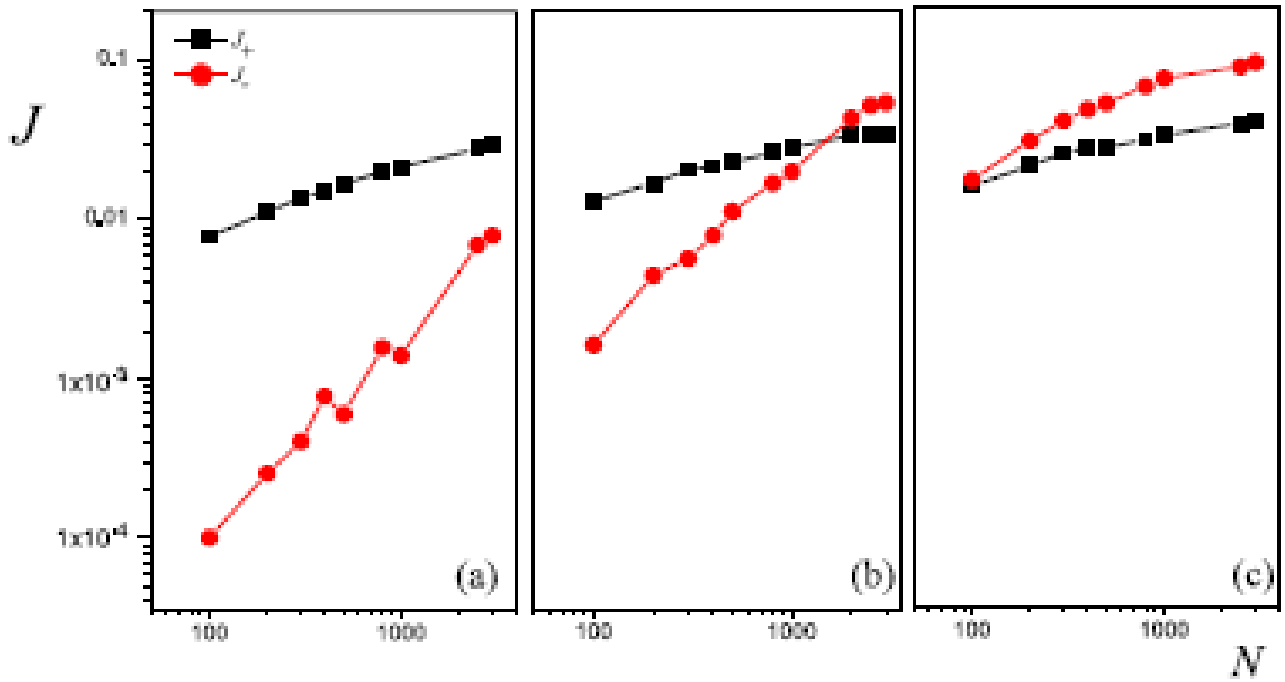

FIG. 3 (color online). Dependence of the total heat flux $J_{\pm}$ on the system size N in the log-log plot for (a) $k_{\mathrm{int}} = 0.05$, (b) $k_{\mathrm{int}} = 0.2$, and (c) $k_{\mathrm{int}} = 0.6$.

$$H = H_A + H_B + \frac{1}{2} k_{\text{int}} (x_{N/2+1} - x_{N/2} - a)^2 + \frac{1}{4} \beta_{\text{int}} (x_{N/2+1} - x_{N/2} - a)^4$$

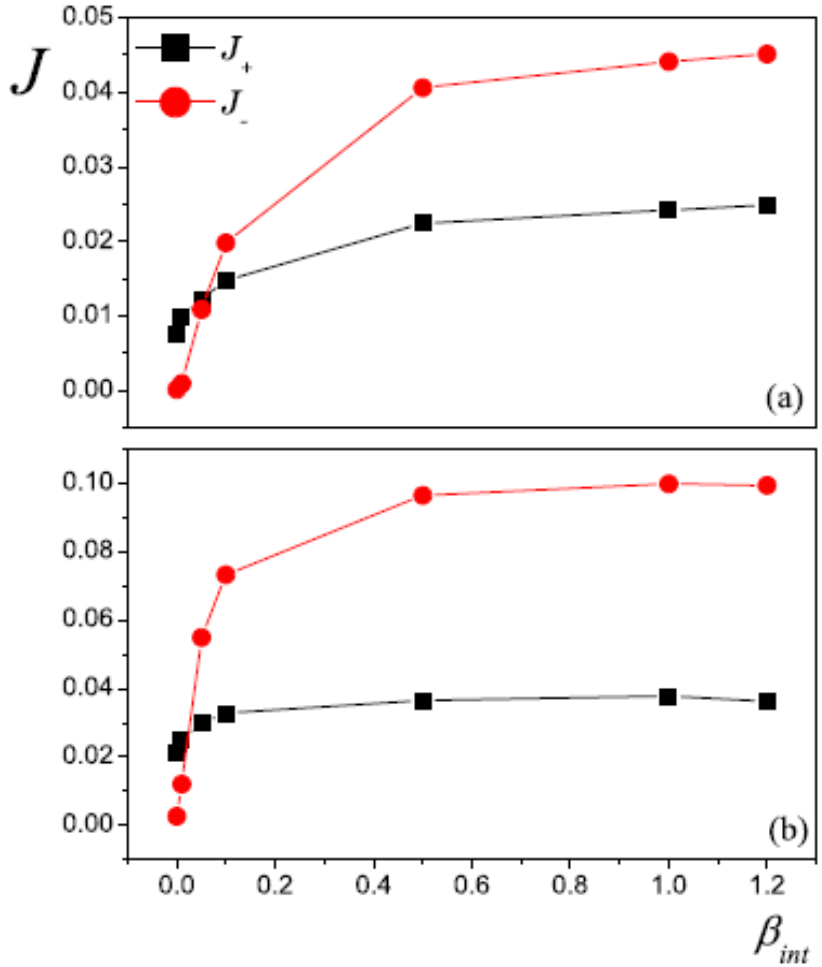

FIG. 4 (color online). Dependence of the total heat flux $J_{\pm}$ on the interfacial anharmonic coupling strength β_{int} for (a) $N = 100$ and (b) $N = 1000$.

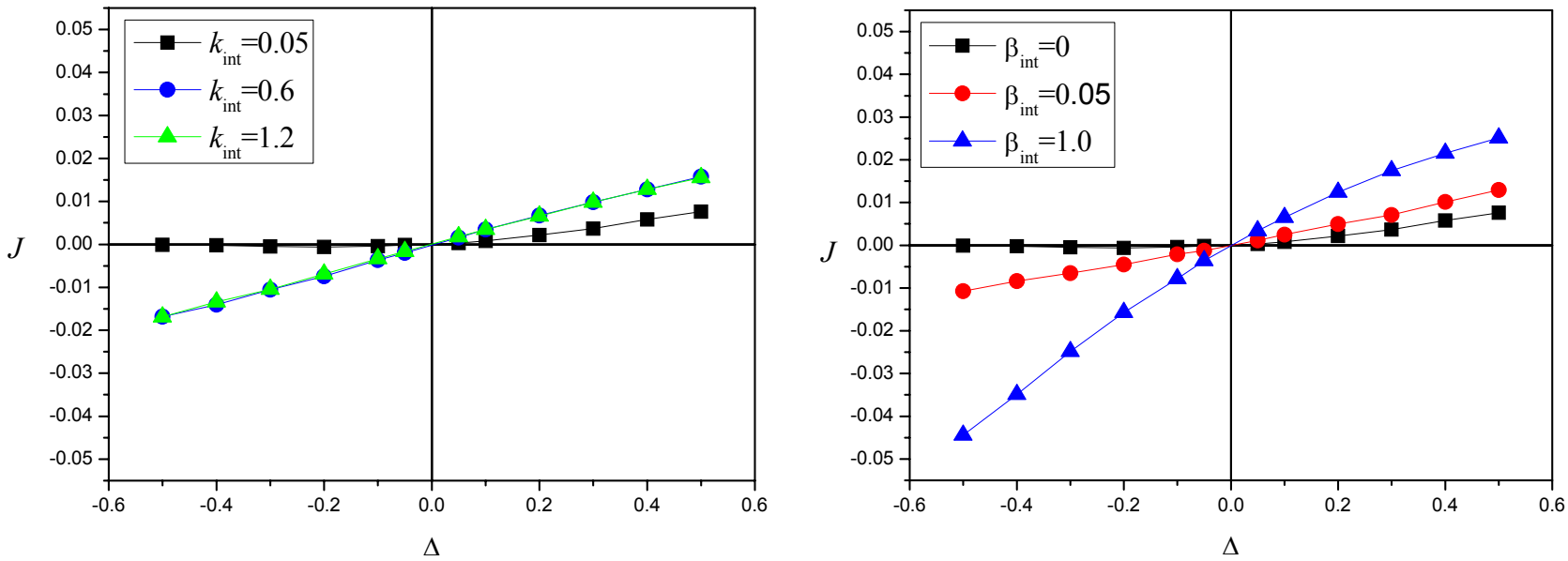

Fig. 5. Dependence of heat flux J on the temperature difference for $T_0 = 0.07$. Here $T_L = T_0*(1+\Delta)$, $T_R = T_0*(1-\Delta)$, $N = 100$.

Reversal of rectification

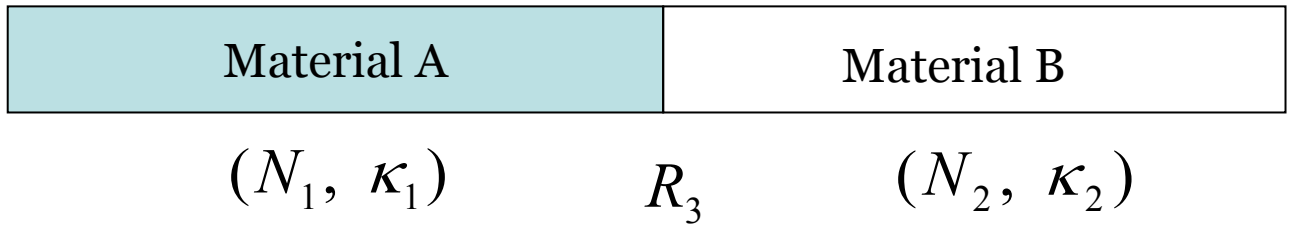

$$R = N_1 / \kappa_1 + N_2 / \kappa_2 + R_3$$

Assume $N_1 = N_2 = N,\ R_3 = 0$

$$\kappa = \frac{2\kappa_1\kappa_2}{\kappa_1 + \kappa_2}$$

Phenomenological explanation

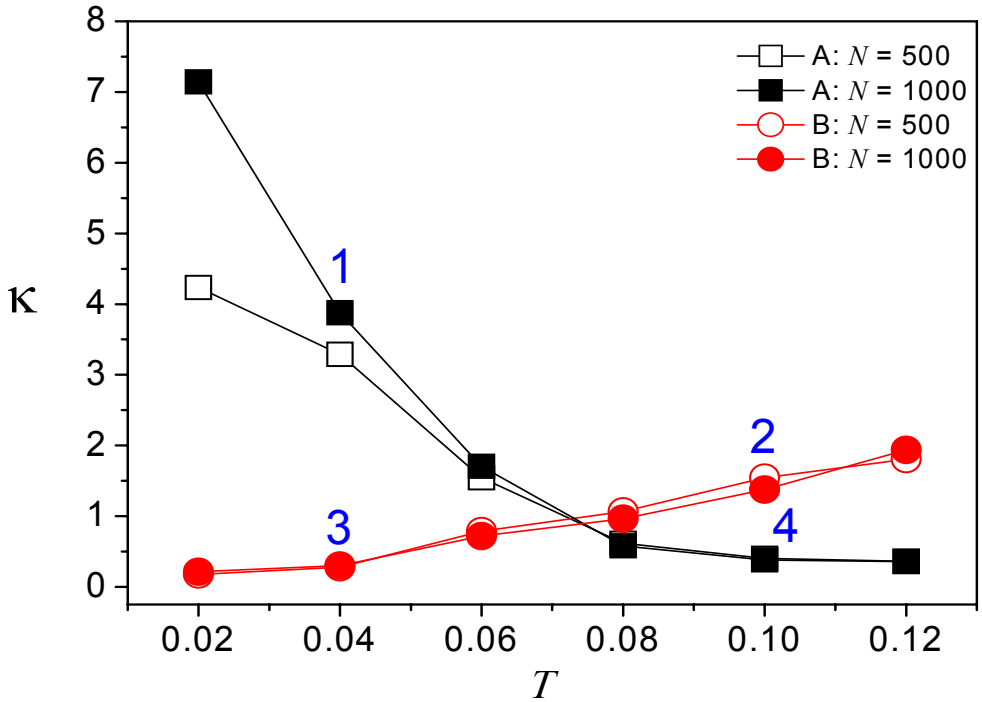

$$J_+ : \kappa_+ = \frac{2\kappa_4\kappa_3}{\kappa_4+\kappa_3} = \frac{2}{\frac{1}{\kappa_4}+\frac{1}{\kappa_3}}$$

$$J_- : \kappa_- = \frac{2\kappa_1\kappa_2}{\kappa_1+\kappa_2} = \frac{2}{\frac{1}{\kappa_1}+\frac{1}{\kappa_2}}$$

$$\because \ \kappa_{1,2} > \kappa_{3,4}$$

$$\therefore \ J_+ < J_-$$

Fig. 6. Dependence of the thermal conductivity κ on the temperature T for segments A and B.

- Experiment

  C. W. Chang, D. Okawa, A. Majumdar, and A. Zettl,
  Science **314**, 1121 (2006).
  C. W. Chang, D. Okawa, H. Garcia, A. Majumdar, and A. Zettl,
  Phys. Rev. Lett. **101**, 075903 (2008).

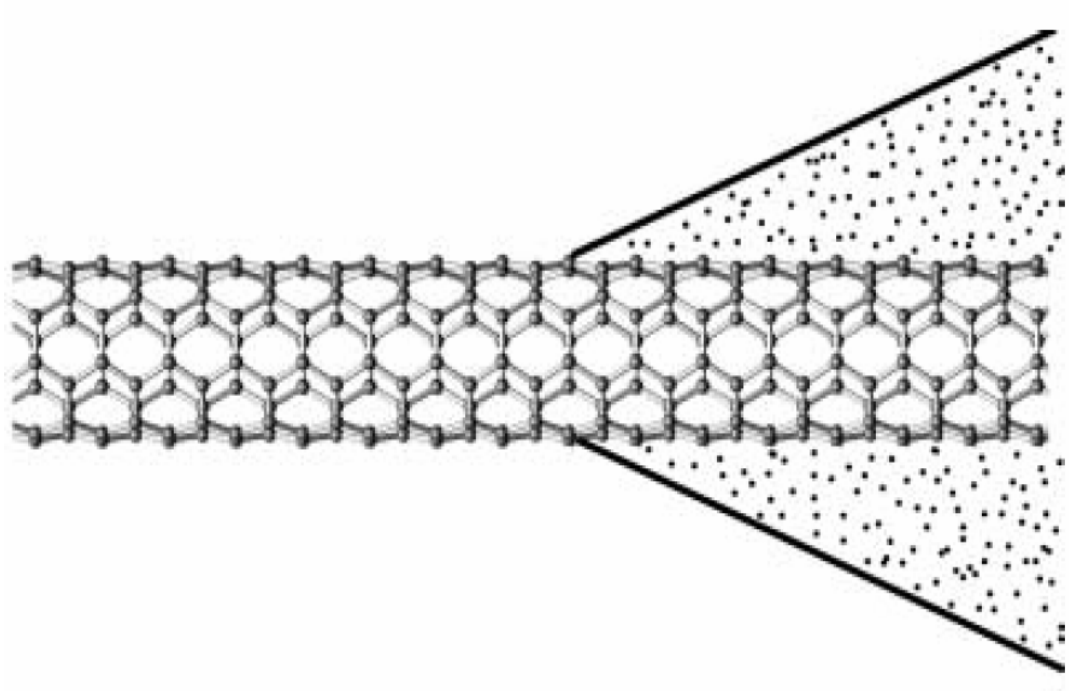

Fig. 1. A schematic description of depositing amorphous $C_9H_{16}Pt$ (black dots) on a nanotube (lattice structure).

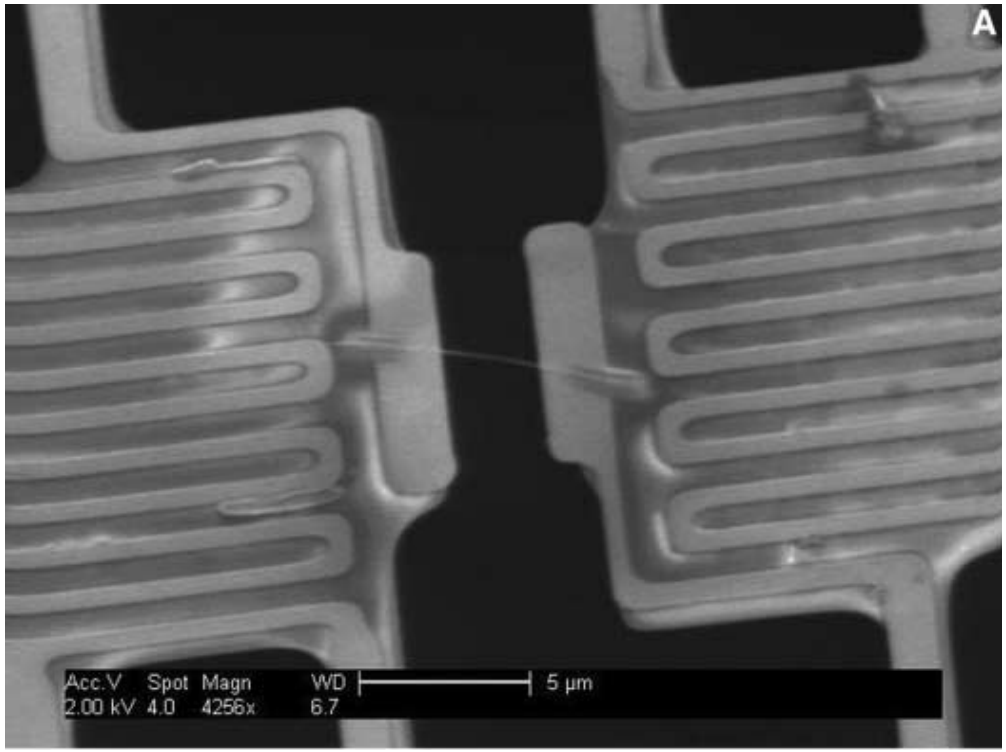

Fig. 2. The SEM image of a CNT (light gray line in center) connected to the electrodes. Scale bar, 5 mm.

Negative Differential Thermal Resistance (NDTR)

Negative differential electrical resistance

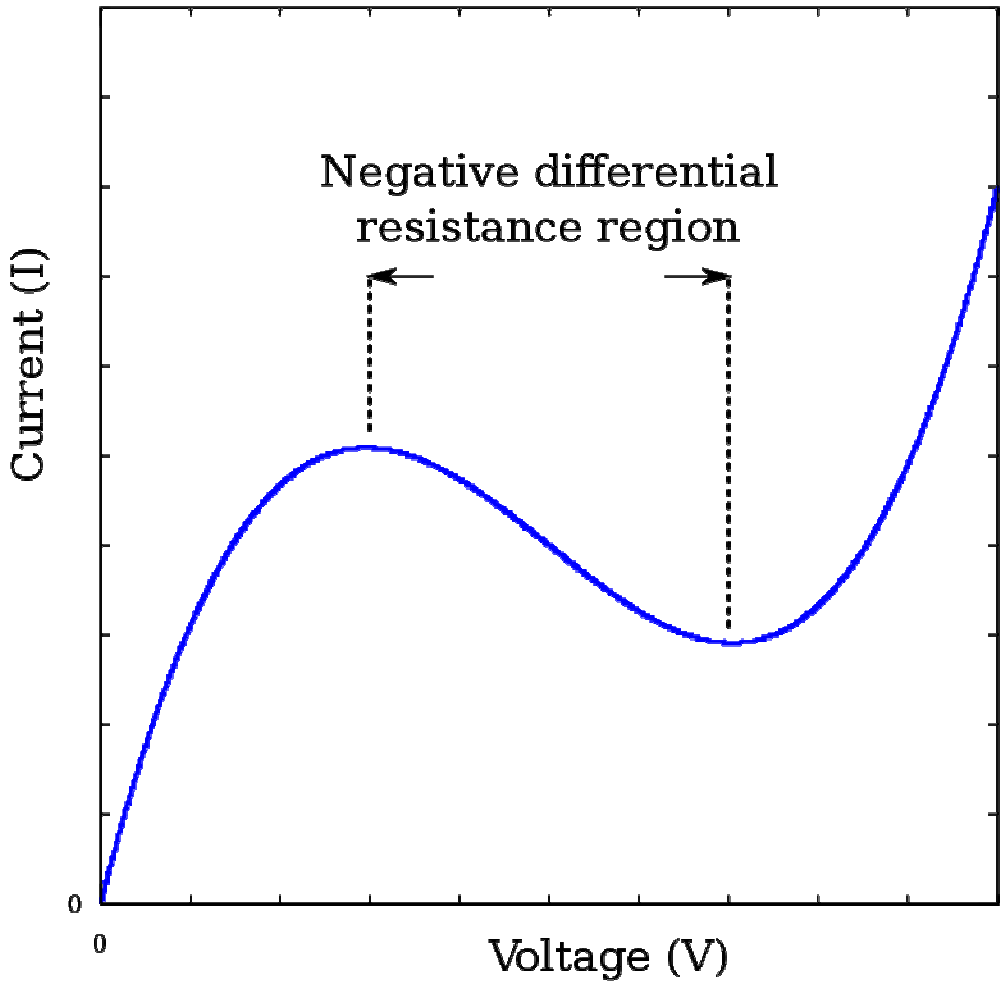

A．NDTR in homogeneous systems

1. With an on-site potential

(a) FK model

$$H_{FK} = \sum_i \left[\frac{p_i^2}{2} + \frac{K}{2}(x_{i+1} - x_i)^2 - \frac{V}{(2\pi)^2}\cos 2\pi x_i \right]$$

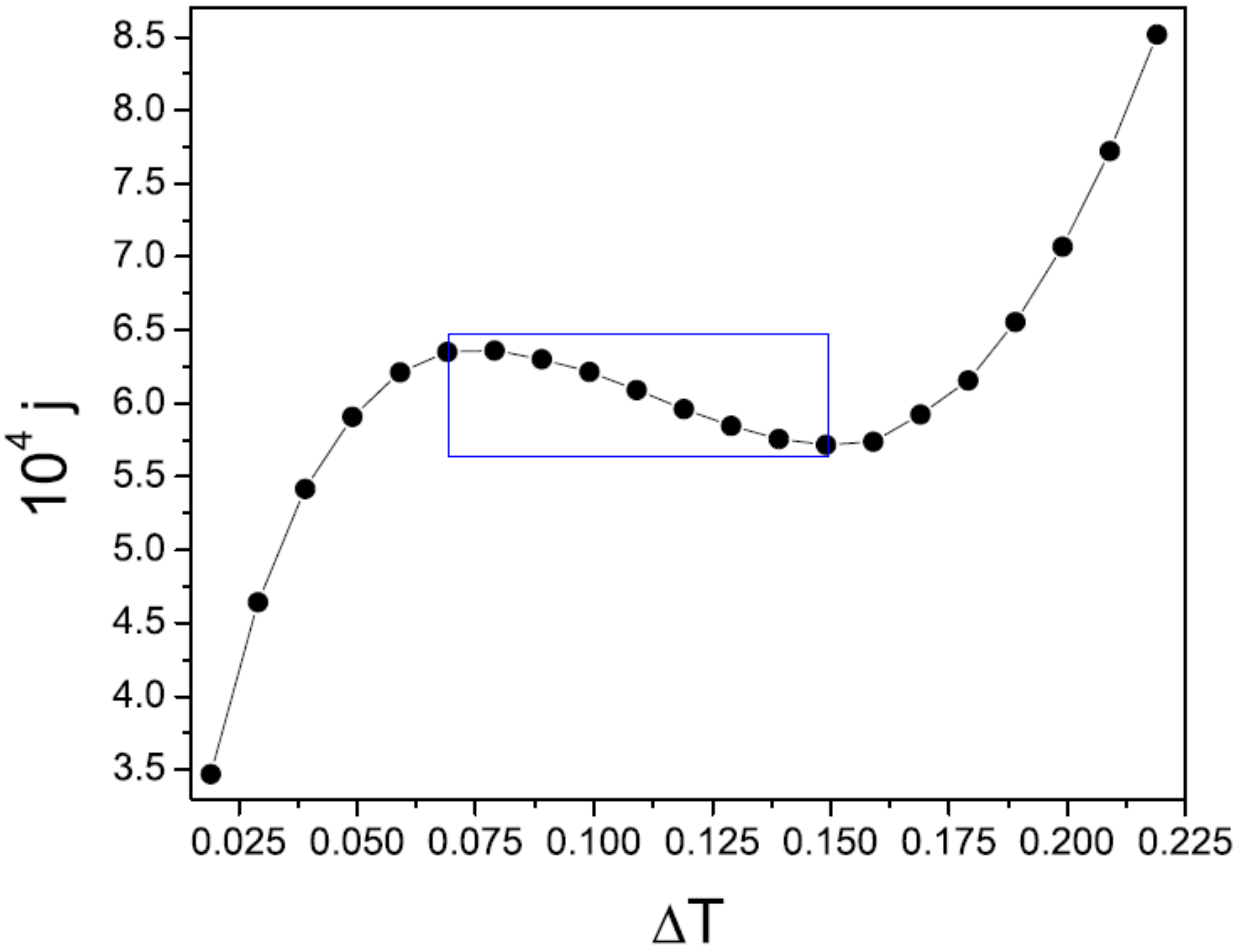

FIG. 1. (Color online) FK model: heat flux j as a function of the applied temperature difference $\Delta T = T_+ - T_-$. NDTR occurs in an intermediate range of ΔT as indicated by the dotted rectangle. Here, $K=0.5$, $V=5$, $T_-=0.001$, and $N=32$.

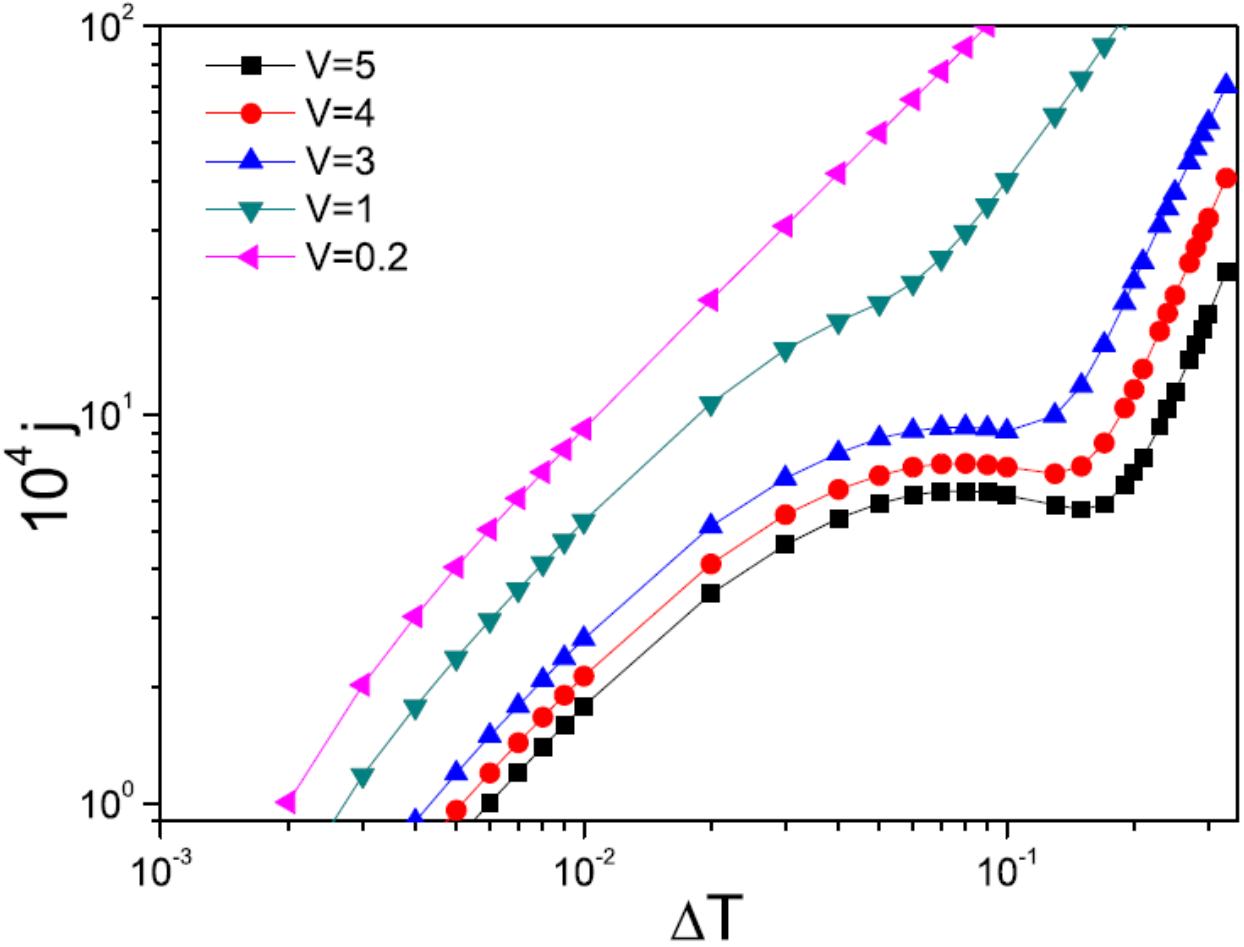

FIG. 2. (Color online) FK model: heat flux j as a function of ΔT for V=0.2, 1, 3, 4, and 5. Here, K=0.5, $T\_$=0.001, and N=32.

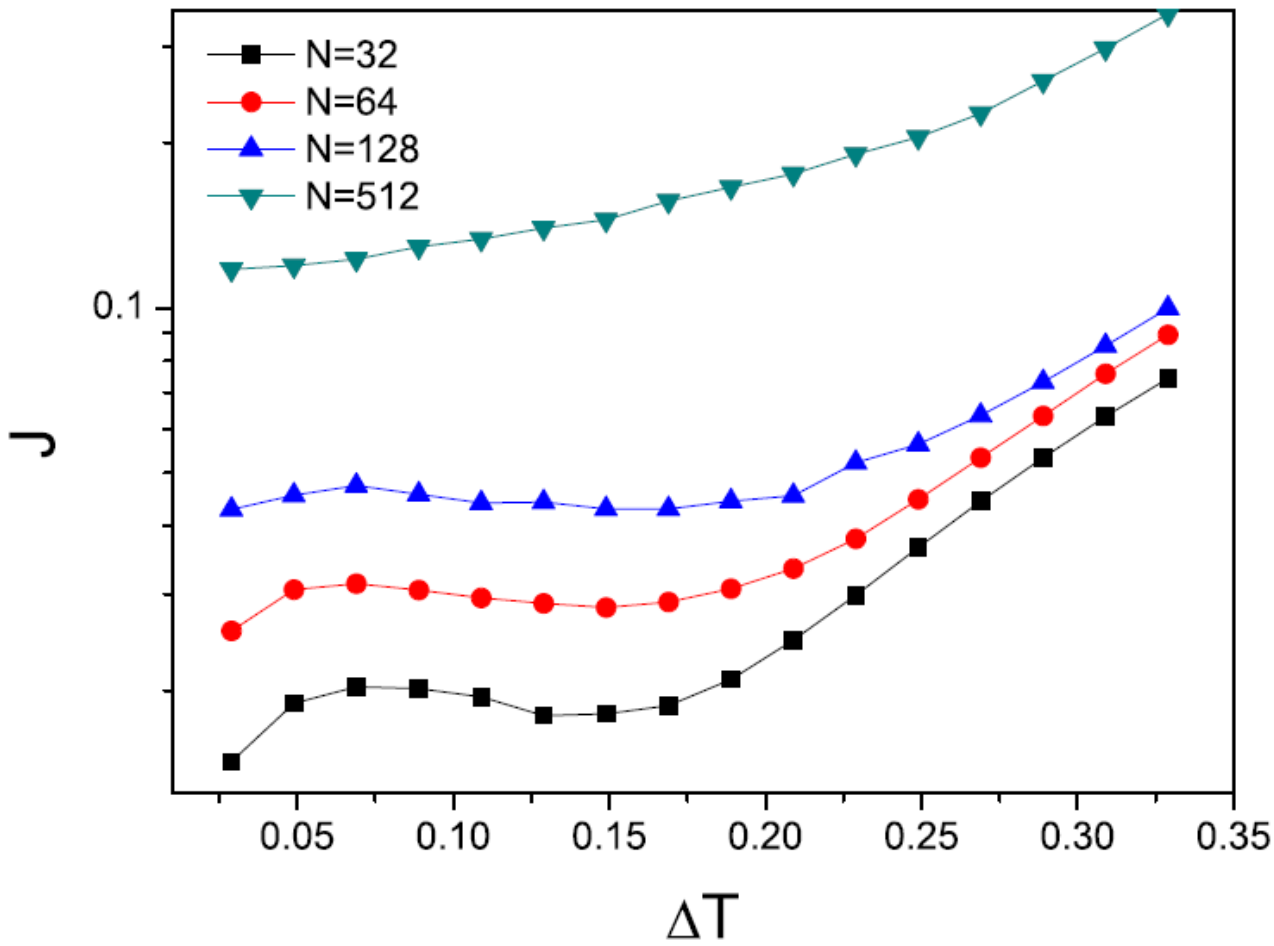

FIG. 3. (Color online) FK model: rescaled heat flux $J=Nj$ as a function of ΔT for $N=32$, 64, 128, and 512. Here, $K=0.5$, $T\_=0.001$, and $V=5$.

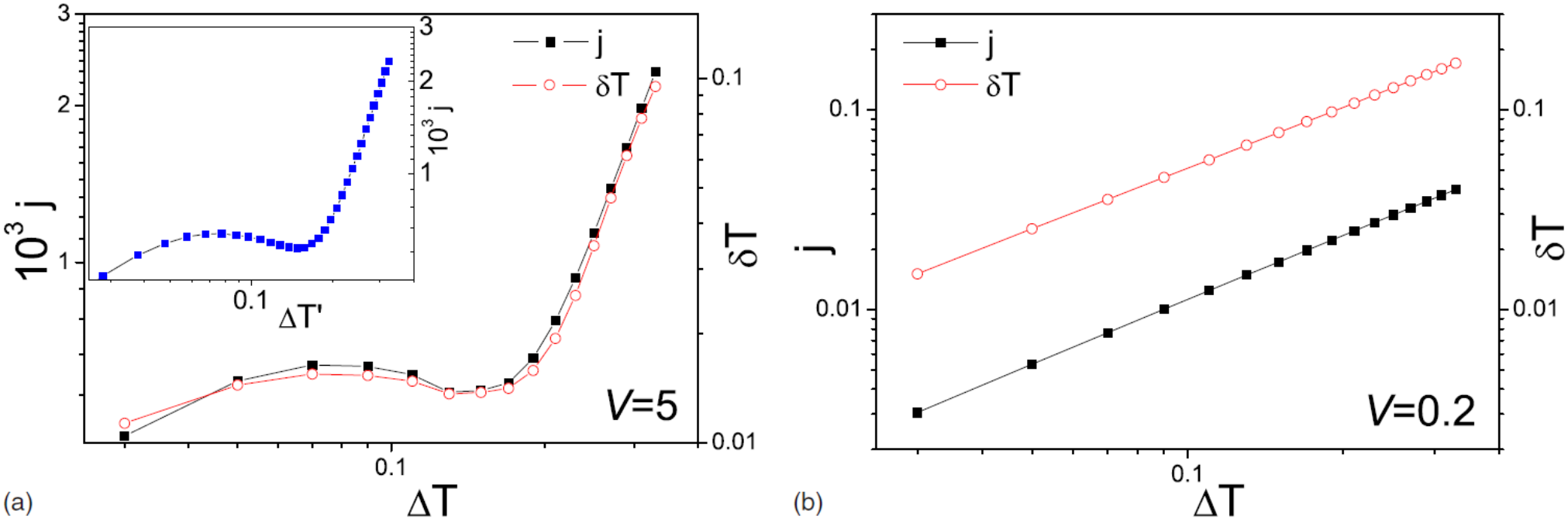

FIG. 4: (Color online) FK model: heat flux j and the corresponding boundary temperature jump δT as a function of ΔT for $V = 5$ (left) and $V = 0.2$ (right). Here, $K = 0.5$, $T_- = 0.001$, and $N = 32$. The inset for the case of $V = 5$ (left) shows a plot of j against the "inner" temperature difference $\Delta T' = T(1) - T(N)$. Note that it also displays the occurrence of NDTR and is practically the same as the plot of j against ΔT. This is because the boundary temperature jumps are typically at least one order of magnitude less than ΔT, meaning that ΔT and $\Delta T'$ are practically the same.

(b) ϕ^4 model

$$H_{\phi^4} = \sum_i \left[\frac{p_i^2}{2} + \frac{1}{2}(x_{i+1} - x_i)^2 + \frac{\lambda}{4} x_i^4 \right]$$

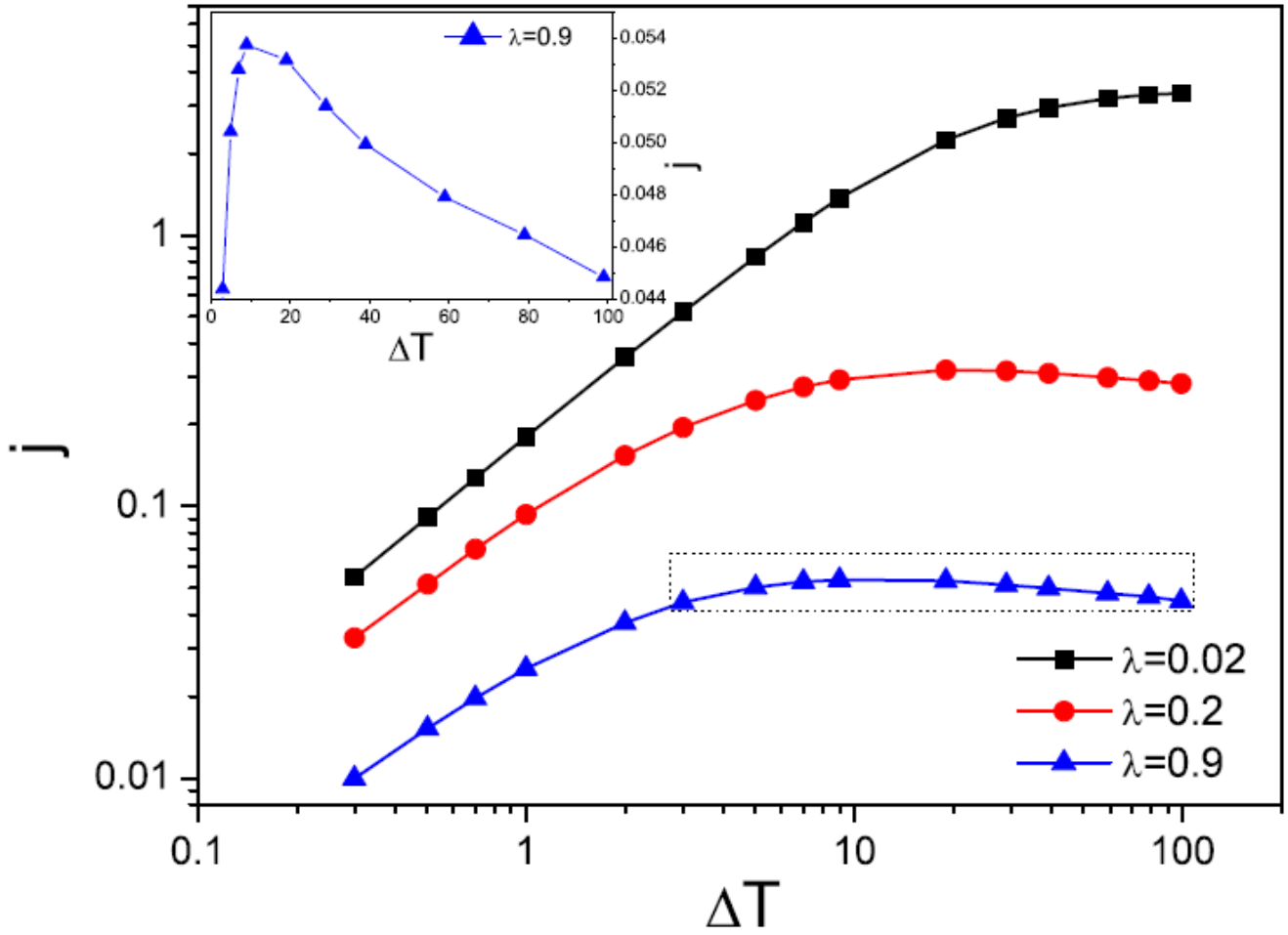

FIG. 5. (Color online) ϕ^4 model: heat flux j as a function of ΔT for $\lambda=0.02$, 0.2, and 0.9. Here, $T\_=1$ and $N=64$. The inset gives an enlarged view of the NDTR behavior within the dotted rectangle for $\lambda=0.9$.

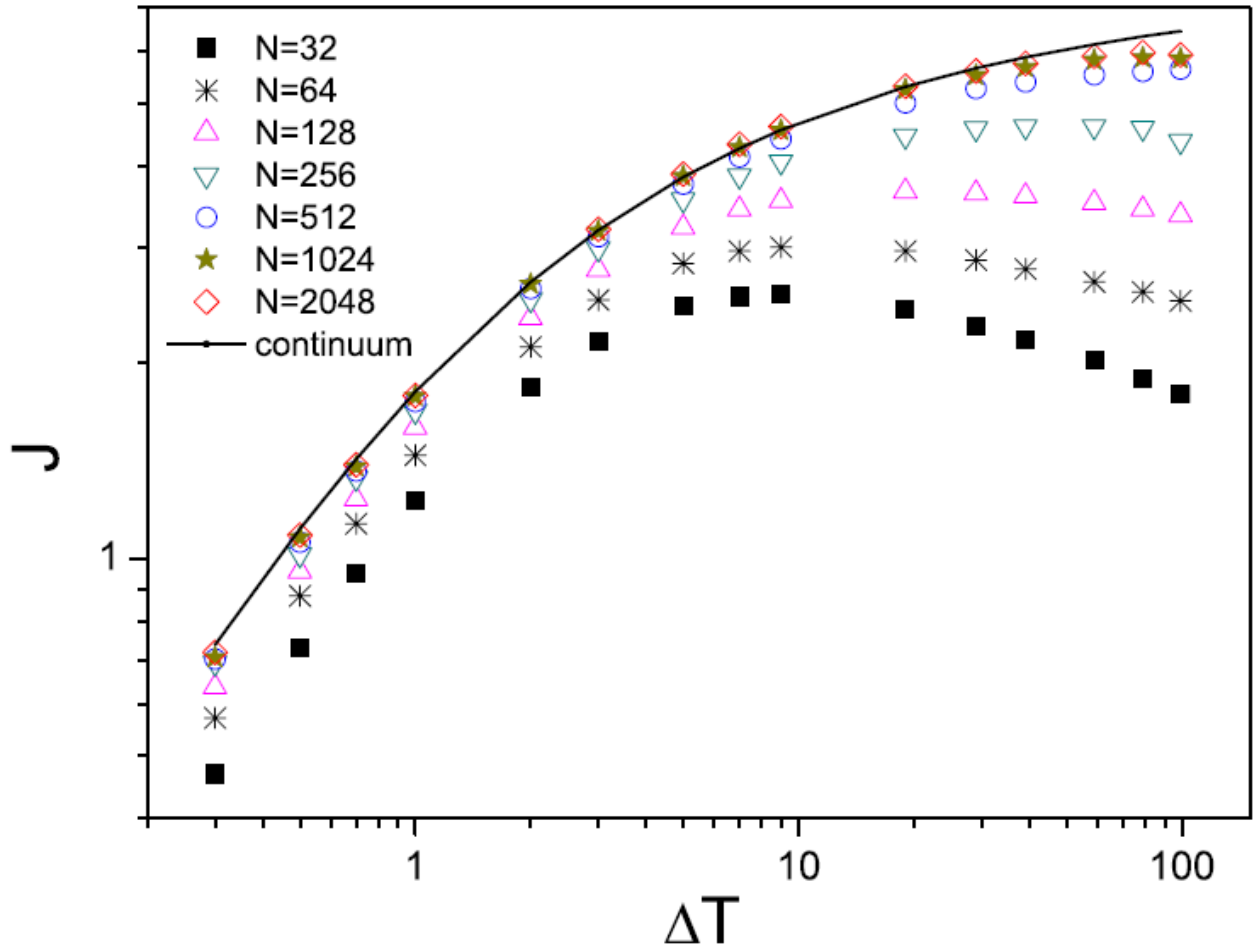

FIG. 6. (Color online) ϕ^4 model: rescaled heat flux $J=Nj$ as a function of ΔT for $N=64$, 128, 256, 512, 1024, and 2048. The solid line depicts the continuum limit as described by Eq. (5). Here, $T\_=1$ and $\lambda=1$.

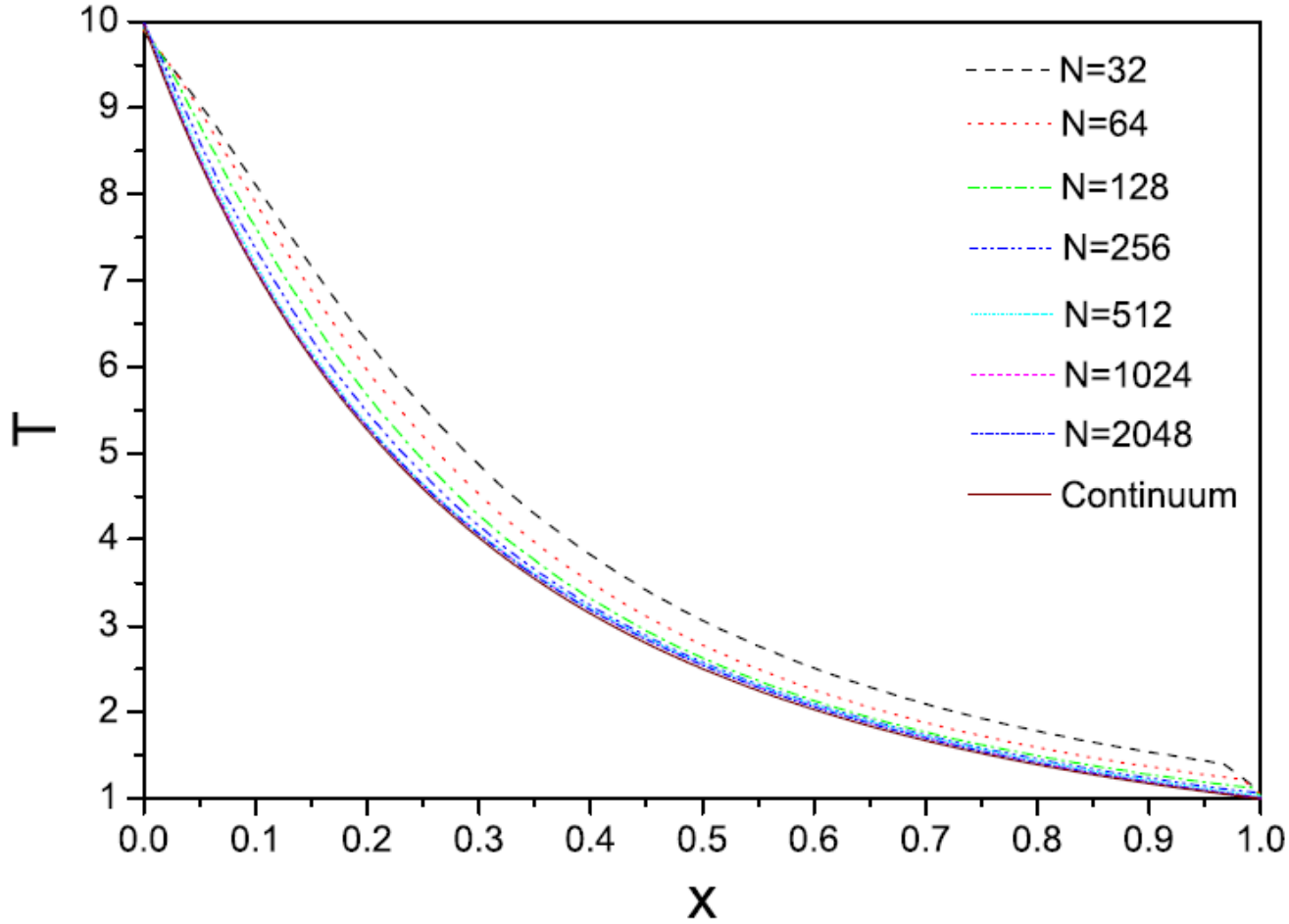

FIG. 7. (Color online) ϕ^4 model: temperature profiles (from top to bottom) for $N=32$, 64, 128, 256, 512, 1024, and 2048, where, for the ith particle, $x \equiv (i-1)/(N-1)$. The solid line depicts the continuum limit as described by Eq. (6). Here, $T_-=1$, $T_+=10$, and $\lambda=1$.

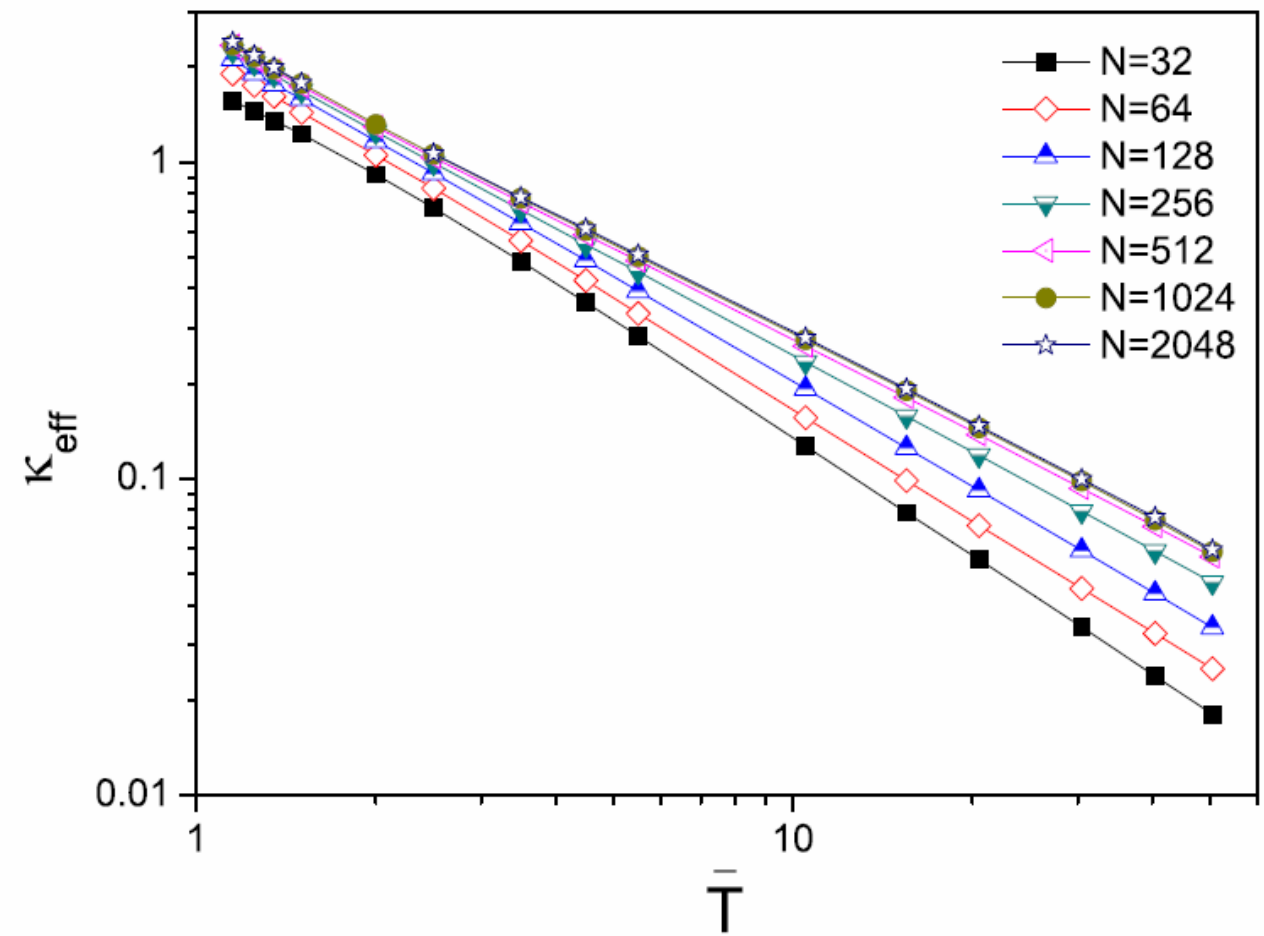

FIG. 8. (Color online) ϕ^4 model: effective thermal conductivity κ_{eff} as a function of the average temperature $\bar{T}=(T_+ + T_-)/2$ for $N=32$, 64, 128, 256, 512, 1024, and 2048. Here, $\lambda=1$ and $T_-=1$, with the covered values of T_+ corresponding to the same values of ΔT in Fig. 6. The straight curves in this log-log graph indicate that the assumed power-law relation in Eq. (7) is valid, even for the nonlinear response regime at $\Delta T \gg 0$ (i.e., $\bar{T} \gg 1$), and that the fitted parameter t is practically zero.

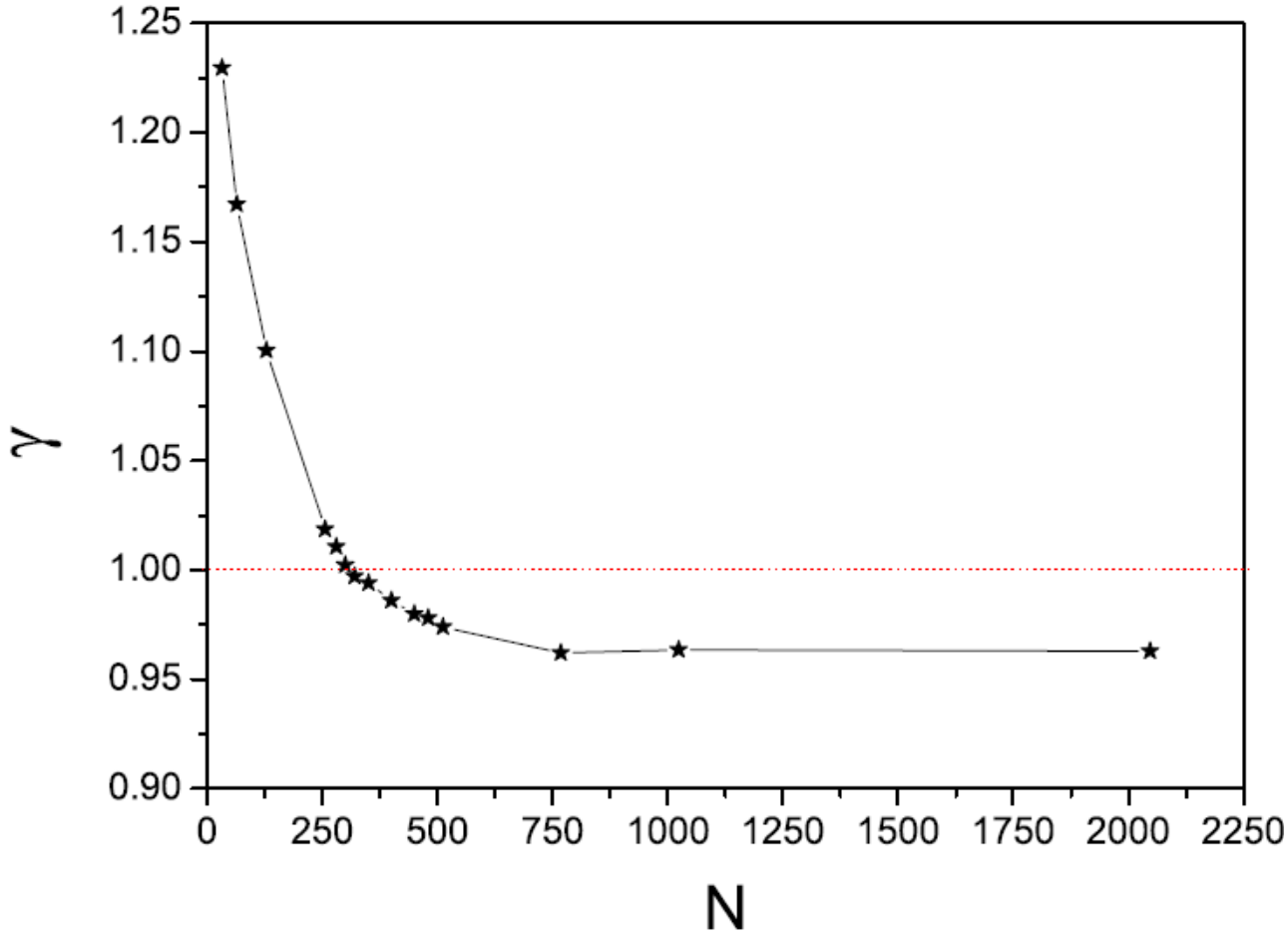

FIG. 9. (Color online) ϕ^4 model: scaling exponent γ as a function of the system size N. The crossover from the existence to the nonexistence of a NDTR regime for increasing N occurs at the critical exponent $\gamma=1$ (dotted line) where $N=N^* \approx 300$.

2. Without an on-site potential: FPU model

$$H_{FPU} = \sum_i \left[\frac{p_i^2}{2} + \frac{1}{2}(x_{i+1} - x_i)^2 + \frac{\beta}{4}(x_{i+1} - x_i)^4 \right]$$

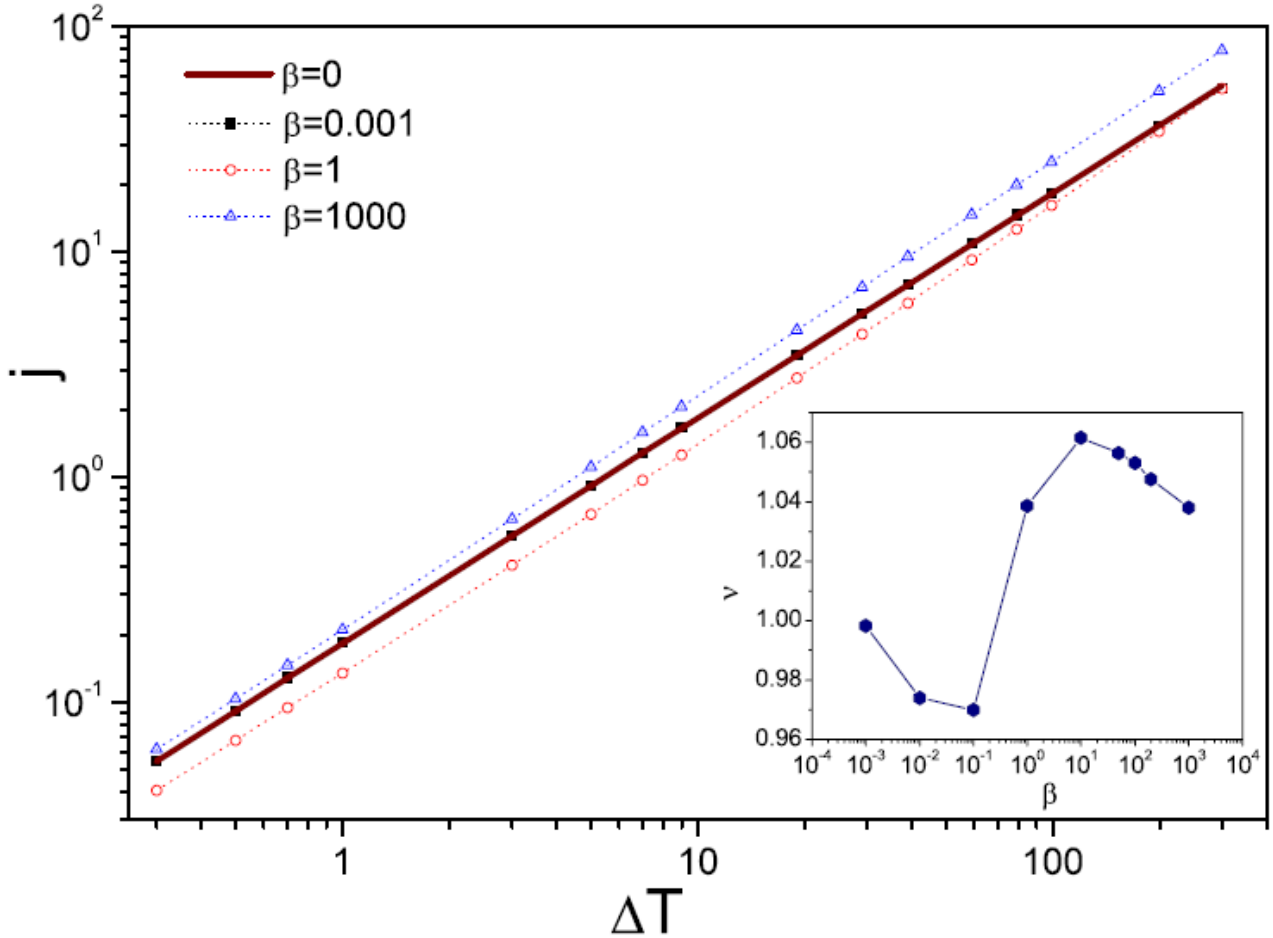

FIG. 10. (Color online) FPU-β model: heat flux j as a function of ΔT for β=0.001, 1, and 1000 in the FPU-β model. Here T_{-}=1. The results are fitted (dotted lines) well by $j \propto \Delta T^{\nu}$. As a reference, the bold solid line depicts the analytical solution for the heat flux in the harmonic limit (β=0), $j=\frac{1+2\chi^2-\sqrt{1+4\chi^2}}{4\chi^3}\Delta T$ (see [23]), where χ is the system-bath coupling. Here, χ=1 was chosen for the numerical simulations. The inset shows that ν varies only within a relatively small range [0.97, 1.06] with the nonlinearity β of the interaction potential.

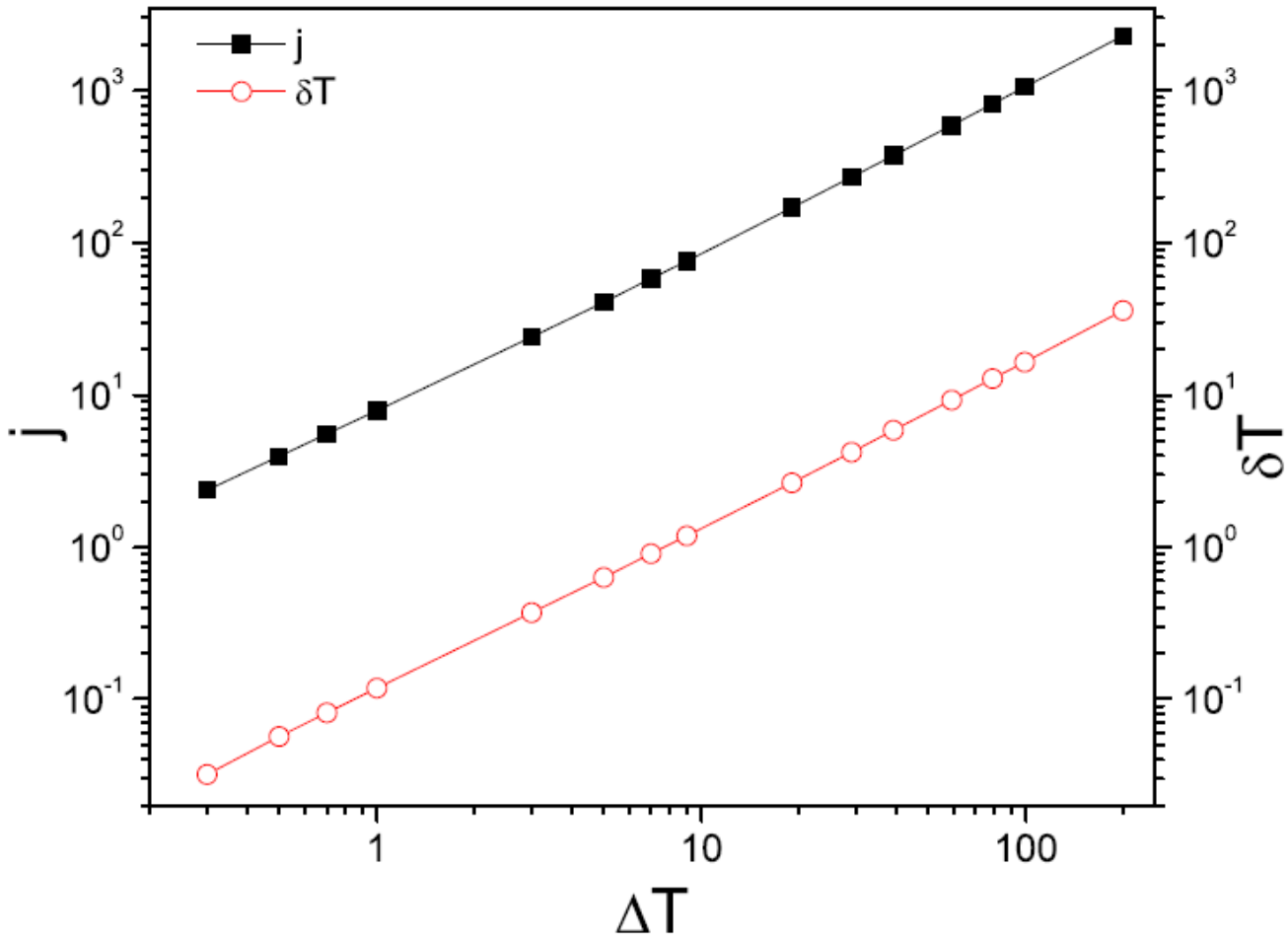

FIG. 11. (Color online) FPU-β model: heat flux j and the corresponding temperature jump δT versus ΔT. Here, $T\_=1$, $\beta=1$ and $N=64$.

3. Without an on-site potential: rotator model

$$H_{rotator} = \sum_i \left[\frac{p_i^2}{2} + K(1 - \cos(x_{i+1} - x_i)) \right]$$

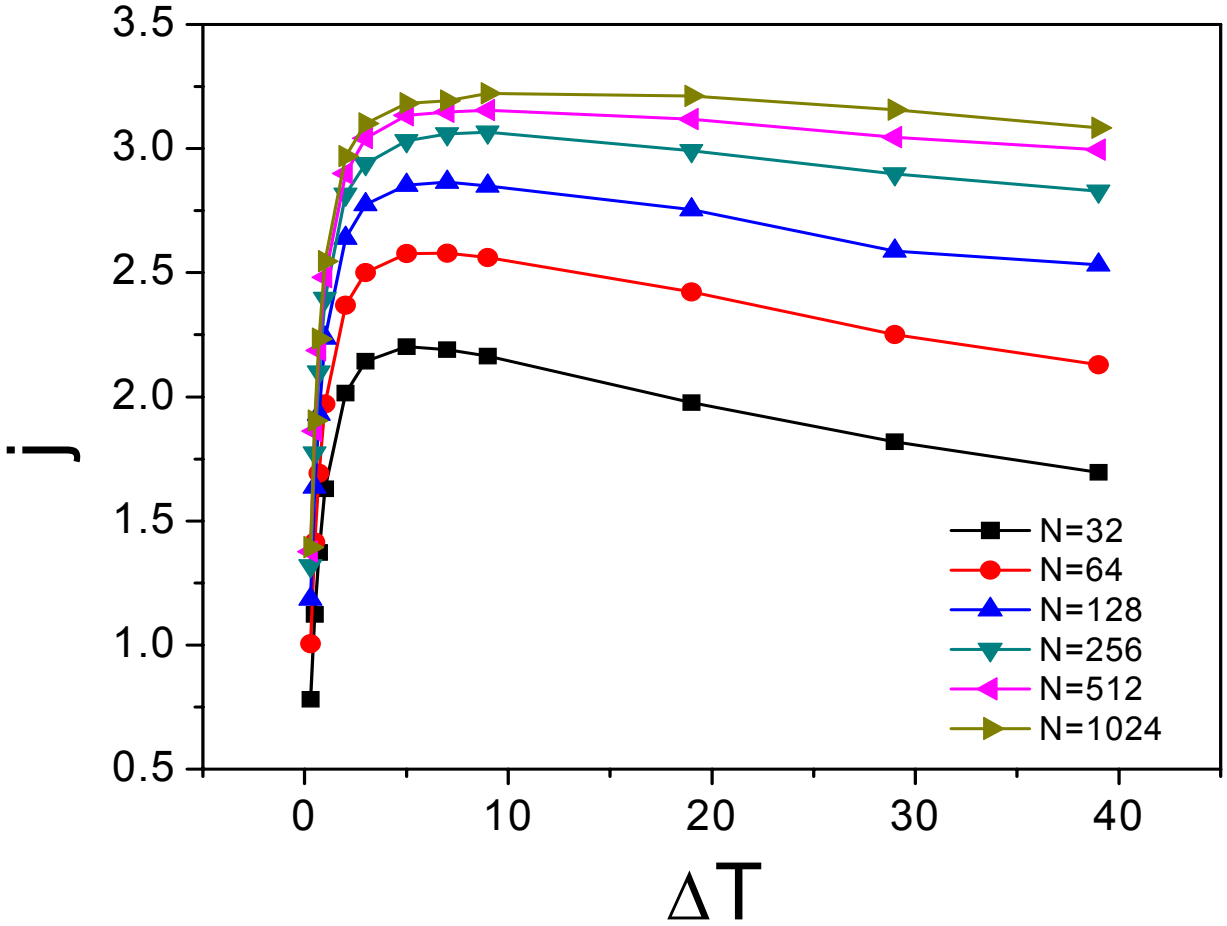

Fig. 12. Rotator model: rescaled heat flux $J=Nj$ as a function of ΔT for N=32, 64, 128, 256, 512, 1024. Here, T_{-}=1 and K=2.

B．NDTR in inhomogeneous systems

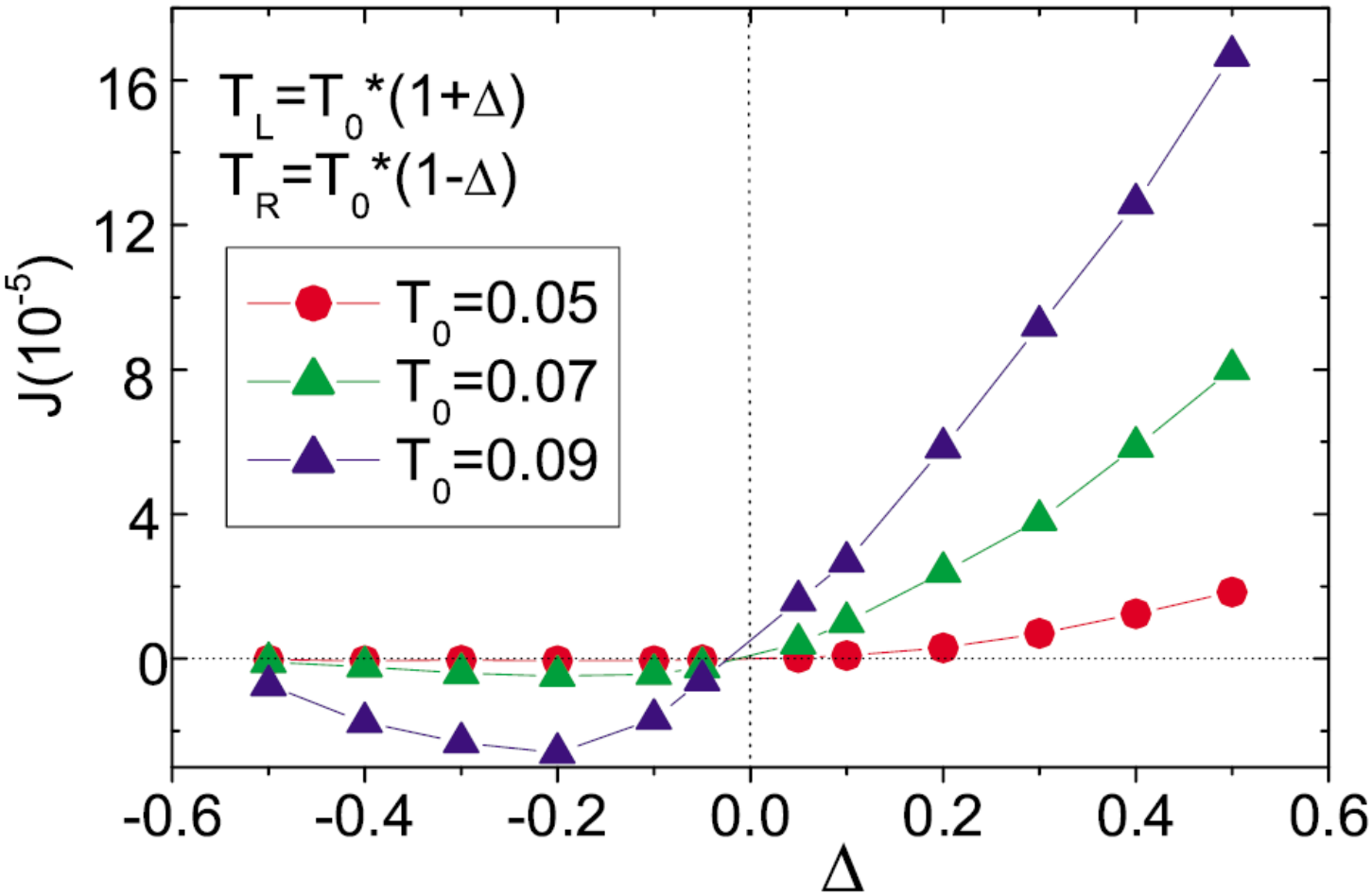

B. Li, L. Wang, and G. Casati, *Phys. Rev. Lett.* **93**, 184301 (2004)

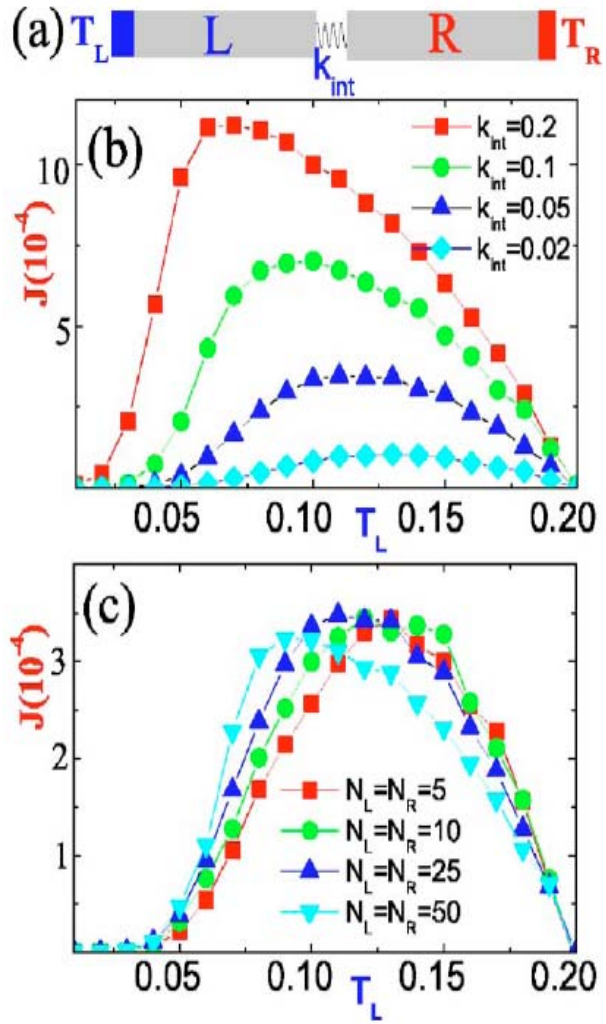

B. Li, L. Wang, and G. Casati, *Appl. Phys. Lett*. **88**, 143501 (2006)

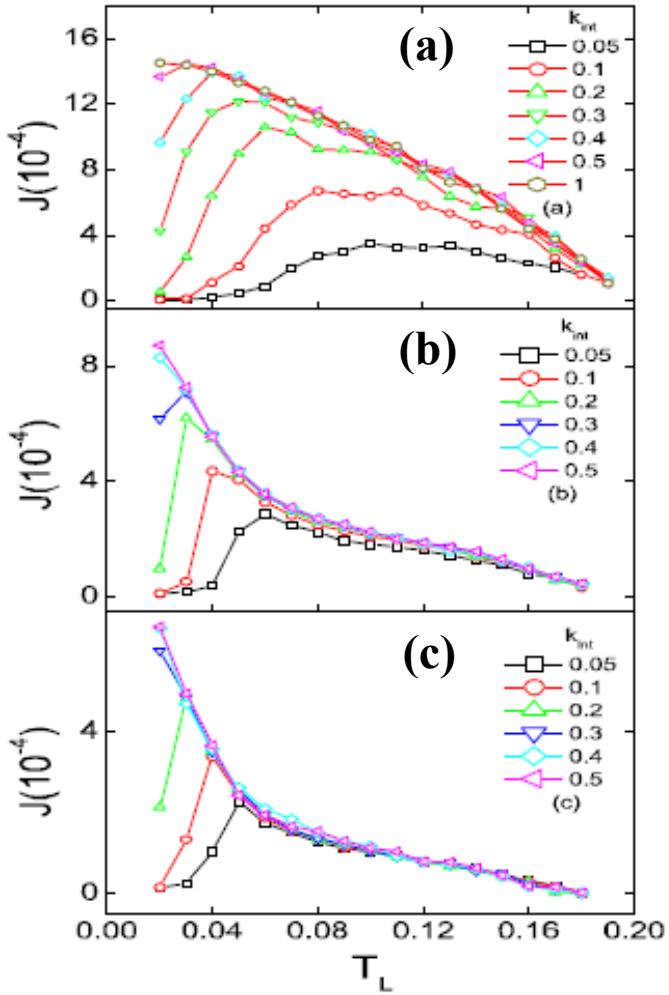

Heat flux as a function of T_L for various k_{int}. (a) $N = 25$, (b) $N = 150$, and (c) $N = 250$.

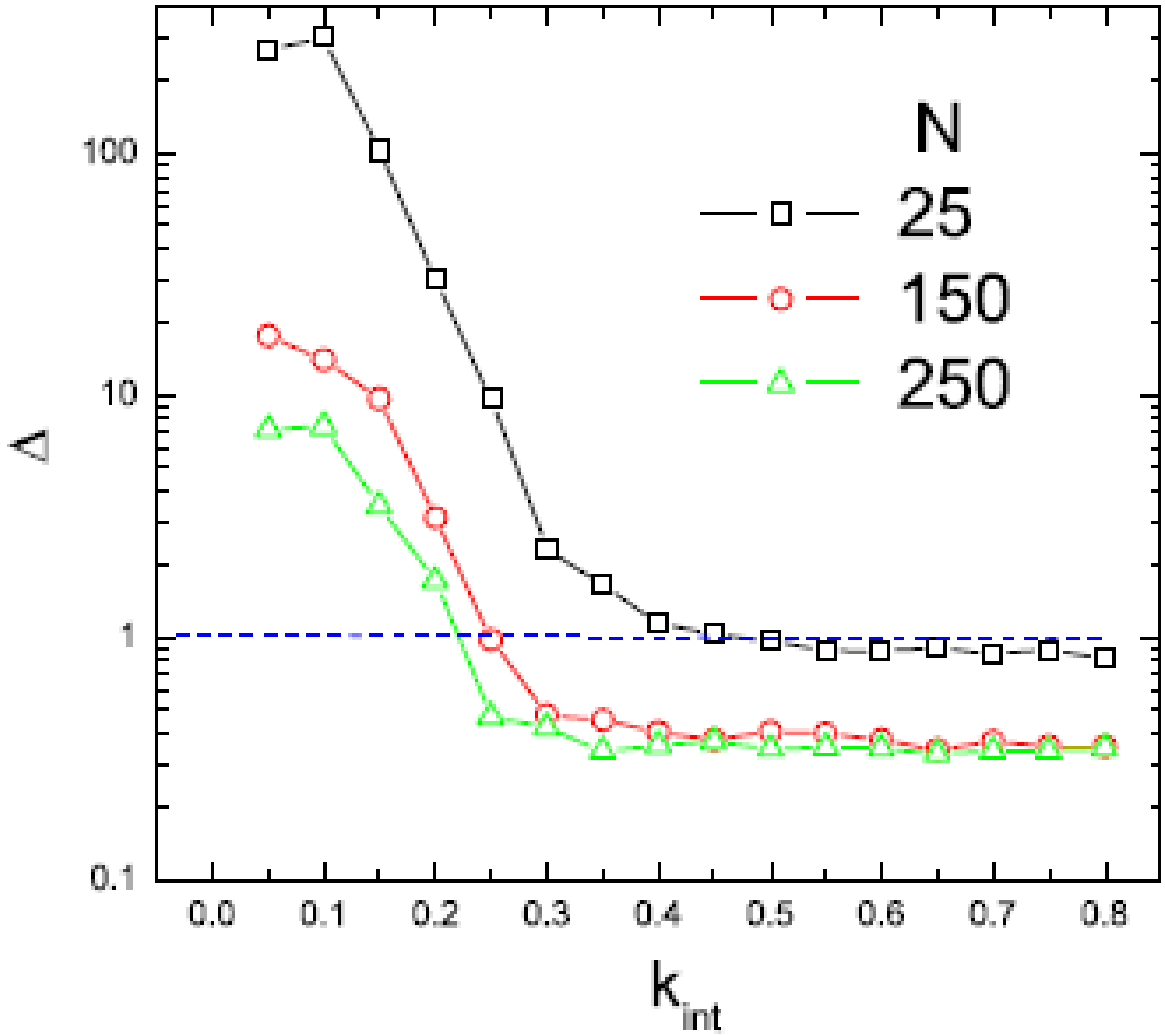

$\Delta = | J_+ / J_- |$ as a function of k_{int} for $N = 25$, 150, and 250.

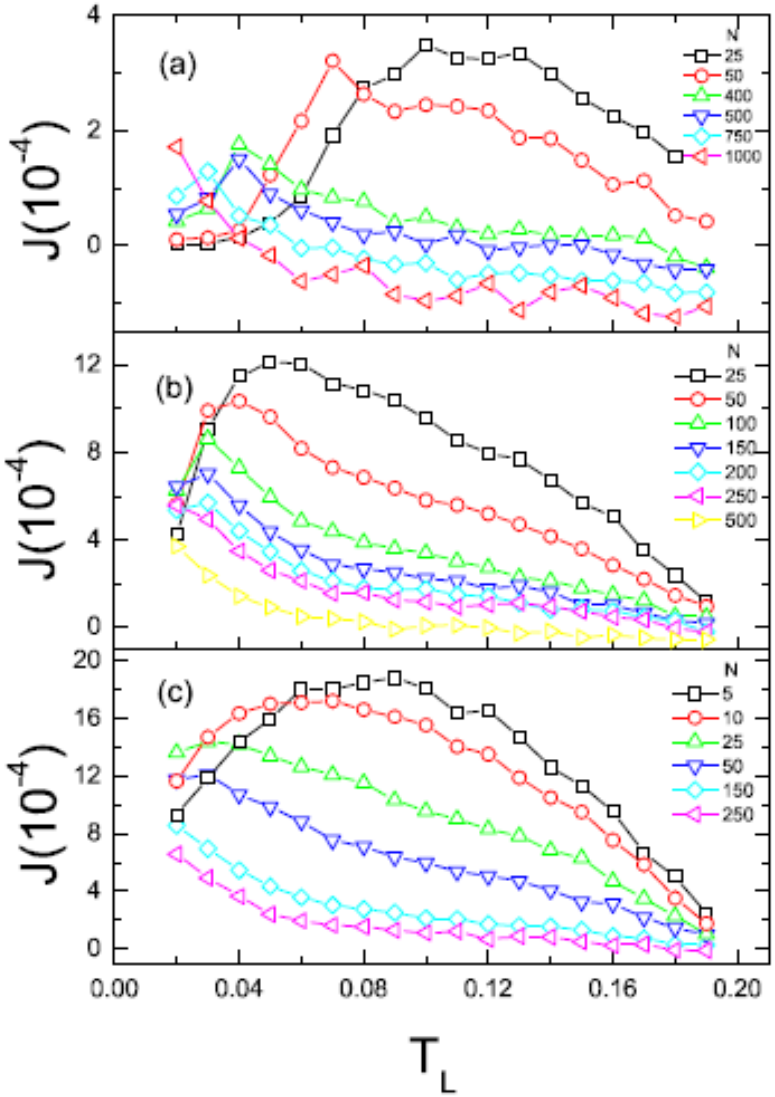

Heat flux as a function of T_L for various N. (a) $k_{\text{int}} = 0.05$, (b) $k_{\text{int}} = 0.3$, and (c) $k_{\text{int}} = 0.5$.

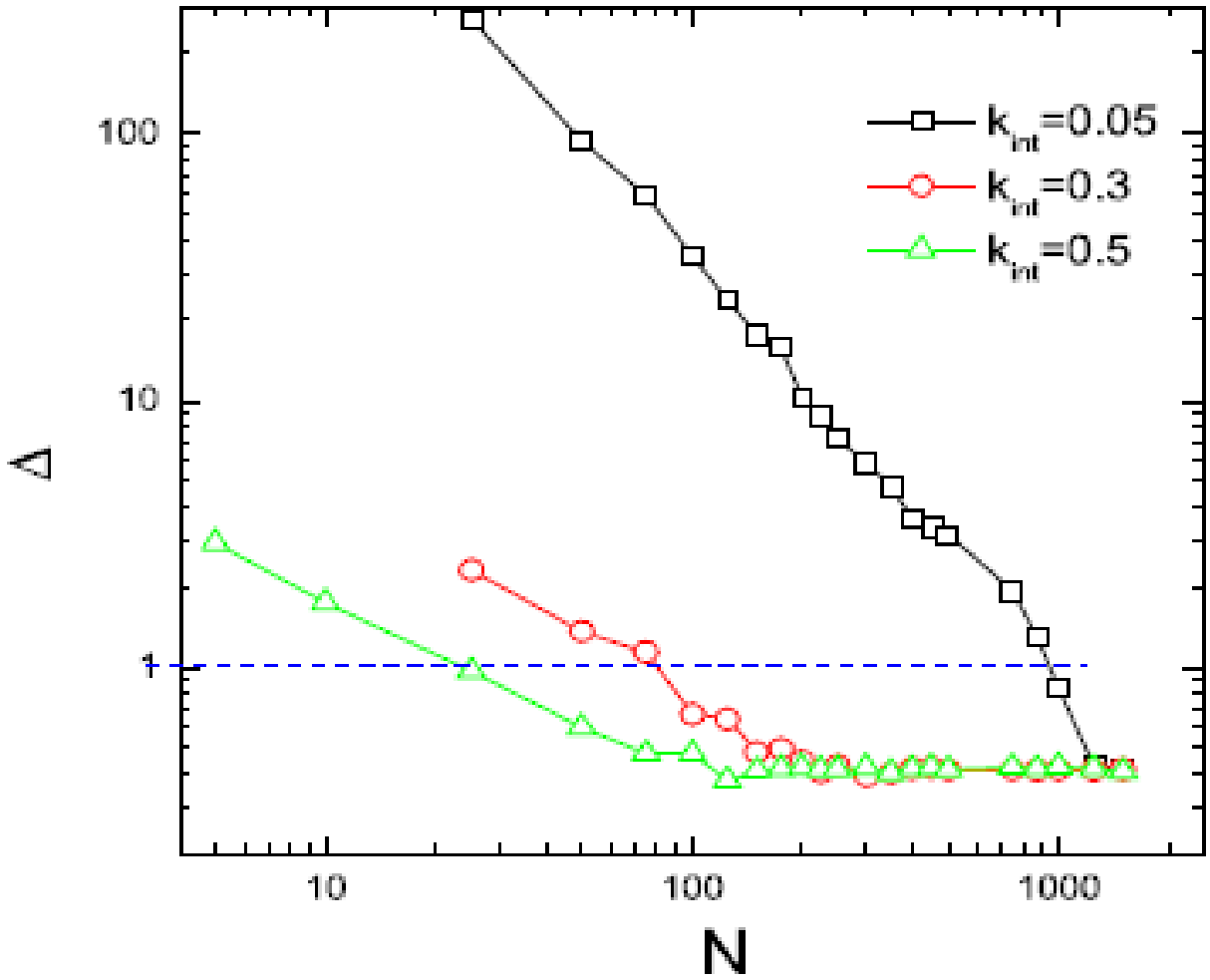

Δ as a function of N for $k_{\text{int}} = 0.05$, 0.3, and 0.5.

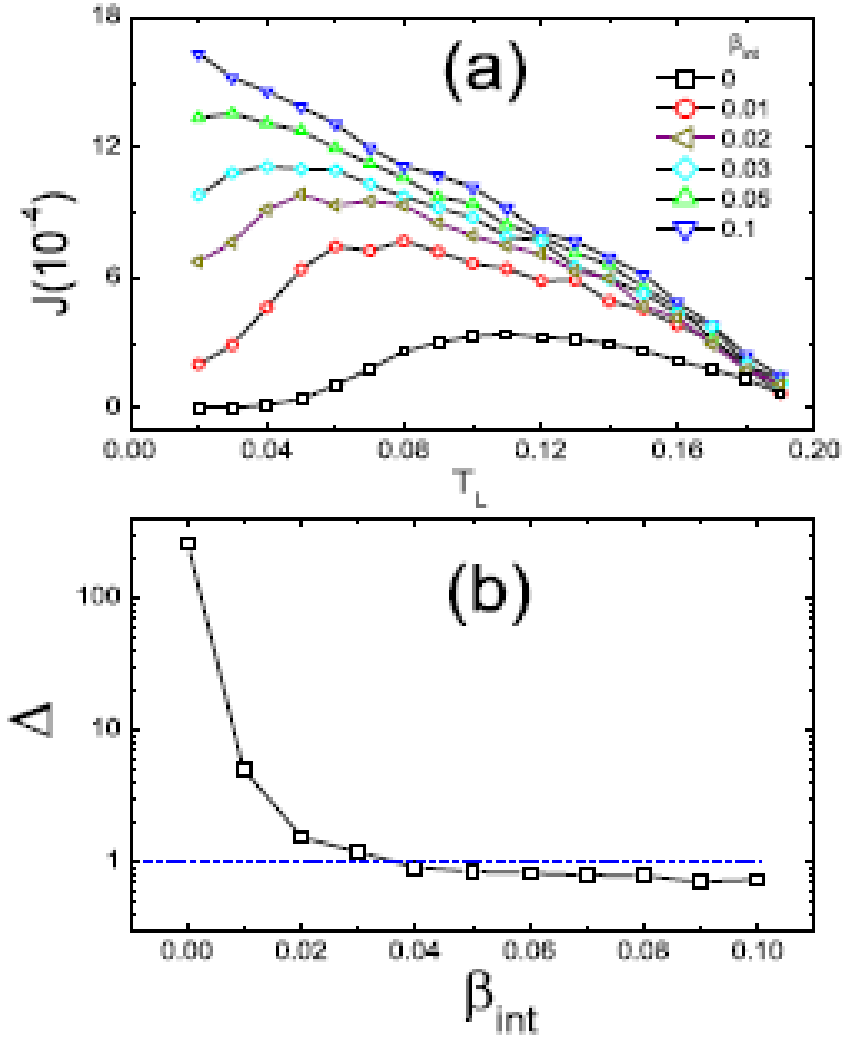

(a) Heat flux as a function of T_L for various β_{int}. (b) Δ as a function of β_{int}. Here $k_{\text{int}} = 0.05$ and $N = 25$.

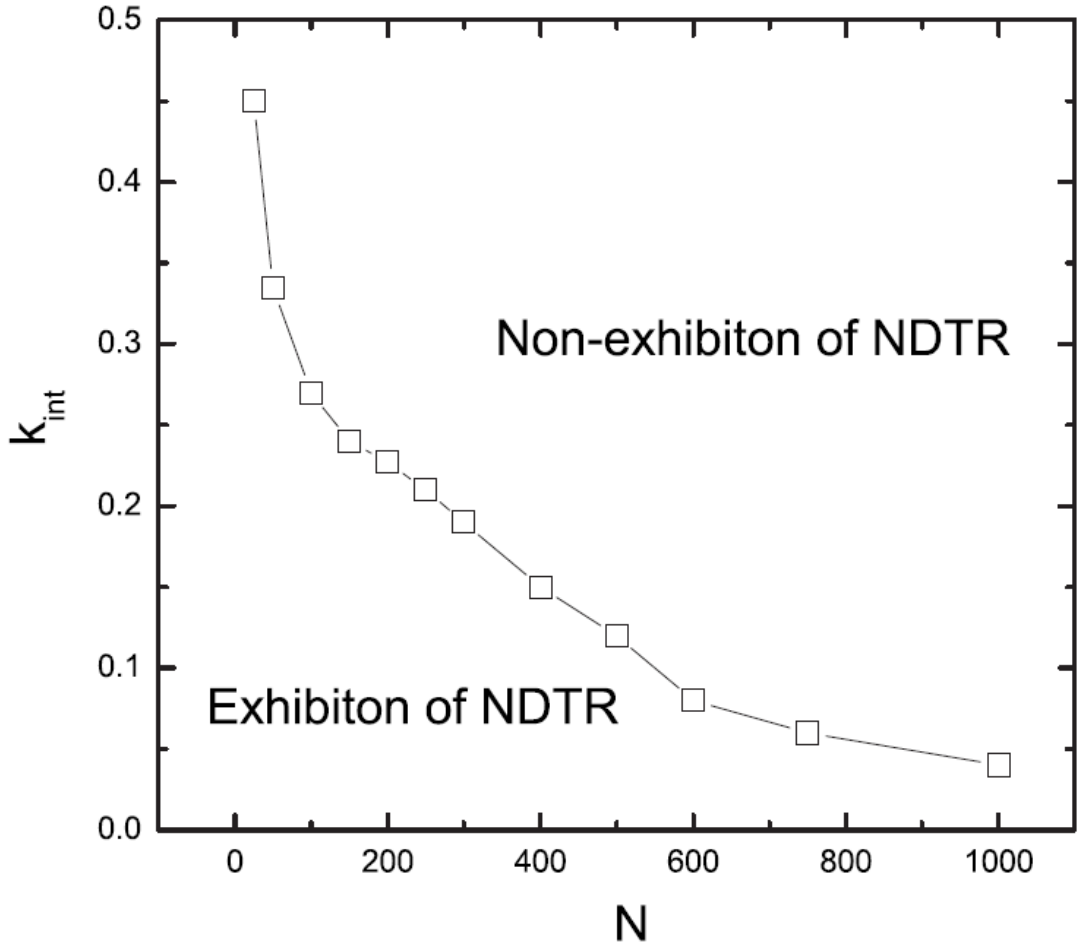

Phase diagram which depicts the range of k_{int} and N for the exhibition of NDTR.

Summary

1. We have found a reversal of the rectification effect in the two-segment FK model.

2. When the coupling of the two segments is weak, phonon band shift leads to $J_+ > J_-$.

3. When the coupling is strong or the chain is long enough, phonon band mixing leads to $J_+ < J_-$.

4. Negative differential thermal resistance (NDTR) occurs both in homogeneous and inhomogeneous systems.

5. Nonlinearity is a necessary condition but not a sufficient condition for NDTR.

6. Normal heat conduction seems to be a necessary condition for NDTR.

7. NDTR depends on the system size. The NDTR regime shrinks as the system size increases.

8. In an inhomogeneous system, NDTR also depends on the interfacial coupling constant. The NDTR regime shrinks as the interfacial coupling constant increases.

Collaborators

B. Q. Ai
S. Buyukdagli
H. K. Chan
A. Fillipov
D. H. He
B. Q. Jin
Y. R. Kivshar
B. Li
H. B. Li
A. V. Savin
Z. G. Shao
P. Q. Tong
L. Wang
B. S. Xie
L. Yang
P. Yang
A. Zeltser
Y. Zhang
H. Zhao
W. R. Zhong

References

I. Asymmetric Heat Conduction

1. B. Hu and L. Yang, *Chaos* **15**, 015119 (2005).
2. B. Hu and L. Yang, *Physica* **A 372**, 272 (2006).
3. B. Hu, D. He, L. Yang, and Y. Zhang, *Phys. Rev.* **E 74**, 060101 (R) (2006).
4. B. Hu, D. He, L. Yang, Y. Zhang, *Phys. Rev.* **E 74**, 060201 (R) (2006).
5. B. Hu, L. Yang, and Y. Zhang, *Phys. Rev. Lett.* **97**, 124302 (2006).

II. Negative Differential Thermal Resistance

1. D. He, B. Buyukdagli, and B. Hu, *Phys. Rev.* **B 80**, 104302 (2009).
2. W.R. Zhong, P. Yang, B.Q. Ai, Z.G. Shao, and B. Hu, *Phys. Rev.* **E 79**, 050103 (R) (2009).
3. Z. Shao, L. Yang, H.K. Chan, and B. Hu, *Phys. Rev.* **E 79**, 061119 (2009).
4. D. He, B.Q. Ai, H.K. Chan, and B. Hu, *Phys. Rev.* **E 81**, 041131 (2010).
5. B.Q. Ai and B. Hu, *Phys. Rev.* **E 83**, 011131 (2011).
6. B.Q. Ai, W.R. Zhong, and B. Hu, *Phys. Rev.* **E 83**, 052102 (2011).
7. W.R. Zhong, M.P. Zhang, B.Q. Ai, and B. Hu, *Phys. Rev.* **E 84**, 031130 (2011).